Diagnosing Drivers of Reservoir Sedimentation in the Western US:
A Case Study of Prineville Reservoir, Oregon

By

Leah C. Bensching

B.S. Santa Clara University, 2016

A Thesis Submitted to the

Faculty of the Graduate School of the

University of Colorado in partial fulfillment

Of the requirements for the degree of

Master of Science

Department of Civil, Environmental and Architectural Engineering

2018

This Thesis entitled: Diagnosing Drivers of Reservoir Sedimentation in the Western US:
A Case study on Prineville Reservoir

Written by Leah C. Bensching
has been approved for the Department of Civil, Environmental and Architectural Engineering

____
Prof. Ben Livneh

____
Prof. Joseph Kasprzyk

____
Dr. J. Toby Minear

____
Dr. Blair Greimann

Date: ________________

The final copy of this thesis has been examined by the signatories, and we find that both the content and the form meet acceptable presentation standards of scholarly work in the above-mentioned discipline.

Bensching, Leah C. (M.S. Civil Engineering)

Diagnosing Drivers of Reservoir Sedimentation in the Western US:

A Case study of Prineville Reservoir

Thesis directed by Ben Livneh and Joseph Kasprzyk

Abstract

There is great need to quantify reservoir storage loss due to sediment. Less than 1% of reservoirs in the US have more than one volume survey. Due to the lack of frequent data collection, a constant rate sediment yield from year to year is often assumed. This study aims to explore the following questions: 1) Can hydrologically-forced sediment algorithms help us advance reservoir sedimentation estimates to improve future planning? 2) To which processes and inputs are reservoir sedimentation estimates most sensitive? 3) What can we learn from models that the linear sediment accumulation assumption fails to assess? It will address these questions through a Sobol Sensitivity analysis a hydrologically forced sediment algorithm ensemble, as well as an evaluation of differences between the hydrologically forced and linear sedimentation assumptions. The hydrologic model used are Variable Infiltration Capacity (VIC) which is coupled with sediment algorithms including the Modified Universal Soil Loss Equation (MUSLE), Hydrological Simulation Program—Fortran (HSPF) and Systeme Hydrologique European Sediment Model (SHE-SED) from within the Distributed Hydrology Soil Vegetation Model (DHSVM). Sediment accumulation will be modeled for Prineville Reservoir near Bend, Oregon.

Dedication

To my Grandmother who was my biggest cheerleader and believed I could accomplish all of my goals.

To my godfather, who was a constant reminder of the love and support sounding me.

Acknowledgements

I would like to acknowledge Dr. Blair Greimann and the US Bureau of Reclamation for collaboration on this work, sharing his expertise, and identification of the case study location chosen for study in this thesis.

I would also like to thank Ben Livneh for being my advisor and guide from my first day at CU. Thank you for your wisdom through this process. Most of all, thank you for your constant encouragement and understanding throughout some tough times.

Thank you, Joe Kasprzyk for joining this research effort and becoming a co-advisor. Your knowledge and guidance greatly benefited the final product.

Most of all thank you to Laura Doyle, my undergraduate advisor, who brought out my love and passion for water resources.

Lastly, I would like to thank my village without whom I would be completing my masters. The CEAE TA's who were my first friends in a new city. My roommates, Lauren, Karen and Heather who helped our apartment feel like a home. Kathy and Brad Arehart for being my second family and welcoming me into their home. My family for support throughout my entire education. The community with in the BAM swim team who helped me find a place to destress. And finally, the doctors who help me learn to cope with a challenging medical condition.

Table of Contents

Chapter 1: Introduction & Background

1.1 Overview

There is great need to quantify reservoir storage loss due to sediment. Typically, the difference between reservoir volume surveys is used to project future sediment loss. However, less than 1% of reservoirs in the US have more than one reservoir volume survey. Due to the lack of frequent data collection, a linearity assumption in the sediment yield is often made for the time between surveys, meaning a constant rate sediment yield from year to year. This assumption does not account for changing climate or the year-to-year variations in hydrology. This study aims to explore the following questions: 1) Can hydrologically-forced sediment algorithms help us advance reservoir sedimentation estimates to improve future planning? 2) To which processes and inputs are reservoir sedimentation estimates most sensitive? 3) What can we learn from models that the linear sediment accumulation assumption fails to assess? It will address these questions through a Sobol Sensitivity analysis of a hydrologically forced sediment algorithm ensemble, as well as an evaluation of differences between the hydrologically forced and linear sedimentation assumptions.

The hydrologic model used is the Variable Infiltration Capacity (VIC) model (Liang et al., 1994). Stewart et al. (2017) coupled sediment algorithms to VIC including the Modified Universal Soil Loss Equation (MUSLE), Hydrological Simulation Program—Fortran (HSPF) and Systeme Hydrologique European Sediment Model (SHE-SED) from within the Distributed Hydrology Soil Vegetation Model (DHSVM). The sediment ensemble used in this study is for suspended sediment load (SSL) only; bed load is not explicitly included in the scope of the study. SSL is modeled as two processes: runoff transport and raindrop impact erosion. The assumption here is that SSL makes up the majority of sediment that settles in a reservoir.

Sediment accumulation will be modeled for Prineville Reservoir near Bend, Oregon. It is fed by the 14133 km^2 Crooked River watershed. The Crooked River watershed is an arid to semi-arid region averaging 12 inches of precipitation per year. Most streamflow is produced by snowmelt in the headwaters. There are two available sediment volume surveys in 1960 and 1998. The model will span this entire period.

1.2 Introduction & Motivation

ASCE 1997 defines the problem of aging dams and reservoirs as one of great relevance to the United States. Reservoirs are vital to support growing populations in the US (Podolak and Doyle, 2015)The boom of reservoir construction between 1940 and 1970 has sustained the water supply of the Western US for decades, providing drinking water, irrigation, flood management and hydropower (Morris and Fan, 1998). However, as reservoirs age, populations grow and the climate changes, there is increased stress on reservoir infrastructure with major concerns for the gradual decrease in storage capacity due to sediment buildup. On a global scale, it is estimated that human activity has doubled sedimentation relative to an undisturbed baseline (Milliman and Syvitski 1992; Vitousek et al. 1997). For reservoirs worldwide, volume loss due to sediment estimates range from 0.1 to 2.5% per year (Jothiprakash and Garg, 2009; Palmieri et al., 2001). To put this into context, a worldwide loss of reservoir storage of 1% would be 70km^3 or twice the volume of Lake Mead (behind Hoover Dam). It is estimated that half of the global reservoir capacity will be lost by 2100 (Kondolf et al., 2014). The average dam in the United States is 60 years old and reservoirs are typically designed to last 50 to 100 years (Morris and Fan, 1998; Palmieri et al., 2001). Many major dams and reservoirs in the US are coming to the end of their design life, motivating a push towards greater understanding of the processes behind reservoir sedimentation to inform and improved mitigation efforts (Morris and Fan, 1998; Podolak and Doyle, 2015).

The importance and usage of a reservoir depends on regional climate, population and land use, but they are most commonly used for a combination of water supply, flood mitigation, hydropower, and recreation (Palmieri et al., 2001). Reservoirs are especially important in the Western U.S. because water supply in the dry season relies on stored snowpack/snowmelt (Pagano et al., 2004; Pierce et al., 2008). In the future, the increasing frequency of extreme events, such as drought and flooding, due to climate change will heighten the need for adequate reservoir infrastructure to mitigate potential flooding and drought (Hamlet and Lettenmaier, 2007). In addition, it is widely accepted that flood events produce the largest amounts of sediment which will increase the projected storage volume loss in reservoirs as flooding is expected to increase (Easterling et al., 2000). The expected shifts in climate will impact not only the storage demand for reservoirs, but also the rate of reservoir sedimentation. Sankey et al., (2017) found that throughout the West, most areas will see an increase in sedimentation due to climatically-forced increases in wild fires. With the expected changes in hydrology and sedimentation, it is important to diagnose and accurately model future reservoir storage loss (Randle and Bountry, 2016).

1.3 Diagnosing Sedimentation

Reservoir sedimentation data are time-consuming and costly to collect, and so there exists relatively limited data needed to fully diagnose the issue of reservoir storage loss. The US Army Core of Engineers (USACE), US Bureau of Reclamation (USBR), US Geological Survey (USGS) and local reservoir managers have collaborated to compile a large-scale reservoir volume survey database called RESSED, which has drastically improved the availability of reservoir survey data. Most reservoirs have only a few (typically one to three) surveys, often decades apart which are inadequate to identify possible changes in sediment accumulation patterns.

Given few available surveys, volume loss due to sediment has been assumed to increase linearly (Graf et al., 2010). This linearity assumption implies a constant rate of sediment input to a reservoir through time, which we will hereafter refer to as sediment ‘yield linearity’. However, even if initial sediment measurements are accurate, changes in hydrologic regime and land cover can drastically change sediment accumulation (Podolak and Doyle, 2015) (Wolman, 1967). For example, wet years can have up to 27 times greater sediment flux than dry years (Inman and Jenkins, 1999). Podolak and Doyle (2015) examined case studies of both under and over estimation in the Redmond Reservoir (Kansas City, MO) and the B. Everett Jordan Lake (Chapel Hill, NC), respectively. The use of linear sedimentation accumulation has the potential to misinform reservoir management strategies and demand capacity due to the incorrect volume estimates.

1.4 Sediment Development and Transport

Sedimentation begins with erosion. The magnitude and characteristics of the eroded material depend on the complex interactions of many factors including topography, geology, climate, soil, vegetation, land use and anthropogenic development (Maidment, 1993). Eroded soil is then transported via surface runoff into streams (Sohoulande Djebou, 2018). Instream sediment can be categorized into bed load or suspended sediment load (SSL).Bed load is solid material that is carried by upward pressure from a combination of fluids (water) and solids from the stream bed (Julien, 2010). It is primarily composed of large particles such as sands and gravels which require more force than that provided by the flow to become fully suspended (Knighton, 2014). SSL is the portion of the sediment load that is suspended nearly continuously by turbulent forces in the flow. Throughout this study, we assume that SSL makes up the majority of the reservoir sedimentation (Maidment, 1993). Suspended sediment is generally composed of fine silts and clays that are brought into suspension by shear forces and turbulent flow (Julien, 2010).

1.5 Sediment Deposition

Once sediment is transported to a reservoir, it may be deposited to the bottom where it replaces potential storage volume. Sediment deposits occurs in two ways, upstream settling and in reservoir settling. Upstream settling can create delta deposits that disrupt the local googology of a river (Annandale et al., 2016). Reservoir settling eliminates storage capacity of reservoirs and is the focus of this work. Not all sediment settles. The fraction (or percentage) of sediment that settles relative to the total sediment input to a reservoir is referred to as sediment *trap efficiency*. The trap efficiency is driven by sediment fall velocity, residence time, reservoir shape and reservoir operation. The most common estimation method for trap efficiency is the Brune equation which uses the reservoir capacity and average annual flow (Brune, 1953).

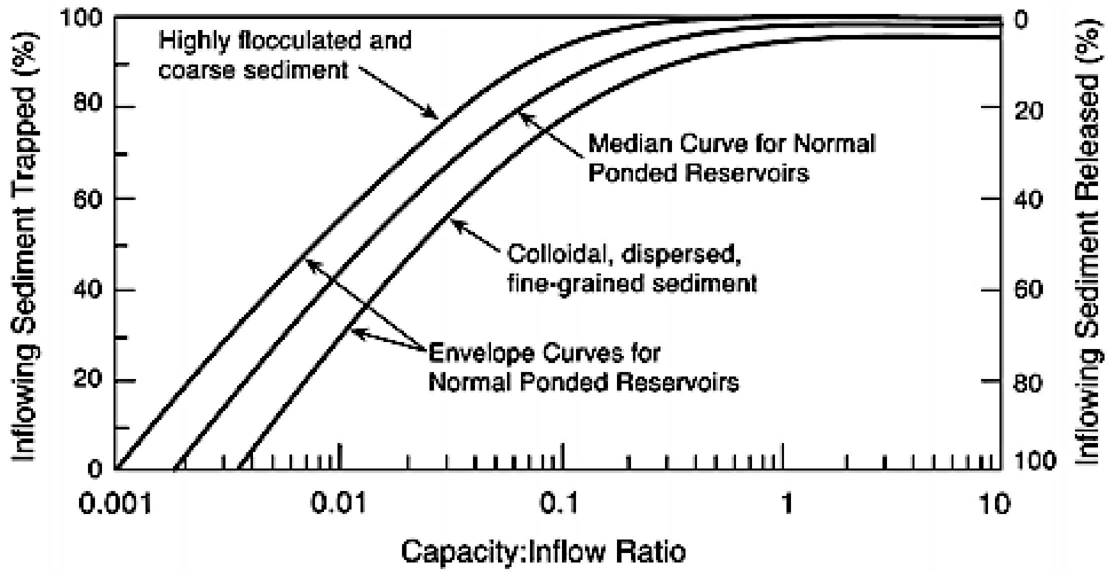

Figure 1.1: Figure from Brune (1953) to estimate sediment trap efficiently based in Capacity inflow ratio and reservoir type.

There have also been a number of other empirical equations that have attempted to estimate the trap efficiency (see Brown, 1949; Churchill, 1947; Dendy and Cooper, 1984; Heinemarm, 1981).

1.6 Sediment Modeling

Catchment sediment yield algorithms have been developed to predict sediment loading across varying spatial scales, temporal resolution and applications from hillslope to catchment scales. They can be physically based, empirical, conceptual or statistical. Many of these sediment yield algorithms rely on hydrologic inputs to drive sediment production. Statistical algorithms rely heavily on in-situ measurements on which to train prediction equations, which can limit their transferability to watersheds that lack sufficient monitoring. Empirical algorithms estimate outputs based on event-based observations, often without underlying theory, which can increase uncertainty in algorithm results when applied outside the training period data. The advantage to empirical algorithms is that they are computationally efficient. Physically based algorithms are the most representative of sediment processes; these algorithms, however, often require estimation of many parameters and thus rely on computationally intensive calibration to estimate suitable values of the parameters.

A variety of algorithms have been developed to model sediment yield, each with their own strengths. The most common sediment yield algorithms are those derived from USLE (Universal Soil Loss Equation) (Odhiambo and Boss, 2004) which include RUSLE (Revised Universal Soil Loss Equation) and MUSLE (Modified Universal Soil Loss Equation) (Williams and Berndt, 1977). The SWAT (Soil and Water Assessment Tool) model uses MUSLE for soil erosion and runoff energy equations for detachment and transport. The combination of MUSLE and SWAT were used to successfully identify which sub-basins were contributing the most sediment to Somerville reservoir in Texas (Sohoulande Djebou, 2018). Yan et al., (2013) use SWAT to quantify how changes in land use effect sediment development. In another study, the ROTO (routing outputs to the outlet) model was developed to simulate water and sediment yields in a large basin for specific applications to reservoirs. The modeled means and standard deviations compared well to observations (Arnold et al., 1995). Minear and Kondolf (2009) developed a model specific for predicting reservoir sedimentation that takes into account processes that are often over looked such as changes in sediment trap efficiency due to sedimentation over time and the construction of multiple reservoirs at different times in a watershed.

Ensembles of sediment yield algorithms have been used previously in Alizadeh et al., (2017) for suspended sediment forecasting and in Himanshu et al., (2017) for prediction of suspended sediment using hydrometeorological data. Sankey et al., (2017) used an ensemble of climate and fire forcing to identify sensitivity of sediment production in western U.S.

watersheds. However, they applied these forcings to a single model, the Water Erosion Prediction Process model. Stewart et al., (2017) developed a hydrologically forced sediment yield algorithm ensemble. The ensemble includes MUSLE (Modified Universal Soil Loss Equation), SHE-SED (Systeme Hydrologique European Sediment Model), HSPF (Hydrological Simulation Program—Fortran), MRC (Monovarietal Rating Curve) and GLM (Generalized Linear Model). The model was validated for instream sediment transport in the Cache La Poudre basin in Colorado. There has yet to be a study that applies an ensemble of sediment yield algorithms to reservoir sedimentation.

1.7 Sediment Management Techniques

There are two common approaches to sediment management: prevention and removal. Prevention includes upstream land management, sediment bypass, sluicing and density current venting. Implementation of large-scale land management practices can be logistically challenging for both landowners and government regulators. In cases where high sediment producing activities such as construction and disforestation are regulated, erosion mitigation increases overall project costs.

Sediment removal practices include dredging, dry excavation and flushing. They can be implemented by reservoir managers and are generally less expensive and time consuming than large scale management practices. Logistically however, currents law in the U.S. prevent wide spread sediment removal. The best strategy for mitigating reservoir sedimentation would include a combination of sediment prevention and removal. Prevention can minimize sediment accumulation, reducing the total amount of sediment needed to be removed (Annandale et al., 2016).

An overarching challenge in sediment management is the limited knowledge of sedimentation quantities in most reservoirs, due to a lack of reservoir surveys. Effective environmental management relies on accurate knowledge of the ecosystem, hydrology and climate. The goal of this study is to explore potential SSL algorithms use for predicting reservoir sedimentation.

1.8 Summary of Chapters

Chapter 2: Methods

Chapter 2 describes the methods used in this model sensitivity study. The chapter starts by describing the selected reservoir including watershed characteristics, flow regime and climate. Model forcing data, sediment observations and streamflow observations are then described. Next, the hydrologic and sediment ensemble algorithms are described. This is followed by the procedure and justification for the sensitivity analysis is explained. Lastly, the method for testing sediment yield linearity is presented.

Chapter 3: Results

Chapter 3 presents the results from the sensitivity analysis for streamflow and the sediment ensemble. First the streamflow sensitivity analysis is presented, and a single parameter set with realistic performance is selected to drive streamflow for use in the sediment ensemble. Next, the Sobol sensitivity analysis for the algorithms with in the sediment ensemble is presented. Finally, the yield linearity assumption of sediment accumulation is assessed based on the sediment algorithm ensemble results.

Chapter 4: Discussion and Conclusion

Chapter 4 summarizes the results of this work and then draws conclusions about the analysis of each sediment algorithm. A conclusion is provided and guidance on future work is suggested.

Chapter 2: Methods

Overview

In Stewart et al., (2017) a new sediment estimation approach was developed through coupling an ensemble of sediment algorithms with a land surface model (LSM), the Variable Infiltration Capacity (VIC) hydrologic framework (Liang et al., 1994). A key benefit of this approach is that a diverse set of sediment algorithms, including DHSVM, HPSF and MUSLE, are driven by the streamflow generated by VIC in response to dynamic climate conditions. Unlike the Stewart et al. (2017) application to a watershed, the hydrologic-sediment framework will be applied to reservoir sedimentation in this research. The primary goal is to improve our understanding of the reservoir sedimentation process. To do so, we conduct a formal sensitivity analysis of key parameters from these widely used sediment algorithms and evaluate the features of simulated sedimentation.

The sensitivity analysis will be performed on the streamflow parameters first, followed by a sensitivity analysis for the sediment parameters. The two stages of the sensitivity analysis allow for independent sensitivity analyses. The streamflow sensitivity analysis is performed first to identify the most accurate streamflow realization to drive the sediment ensemble with the goal of the streamflow driving the sediment algorithms being as realistic as possible. A set of realistic performing parameters will then be used to drive streamflow for the sensitivity analysis on the ensemble of sediment algorithms. The outcome of this research will be an improved understanding of physical and empirical modeling parameters associated with streamflow-sediment modeling. The key questions posed here include: 1) Can hydrologically-forced algorithms help us improve reservoir sedimentation estimates useful for future planning? 2) To which processes and inputs are reservoir sedimentation estimates most sensitive? 3) What can we learn from models that the linear sediment yield assumption fails to assess?

2.1 Study Area

The study area, Prineville Reservoir, in central Oregon, was selected from among several reservoirs suggested by Blair Greimann, our USBR collaborator. Prineville Reservoir is representative of the typical data availability and arid to semi-arid climate of many reservoirs across the west. It was filled following construction of Arthur Bowman Dam in 1960 (Eggers, 2003). The reservoir is fed by the 14133 km^2 Crooked River watershed located in the Deschutes River basin, a map of which is seen in figure 2.1. The Prineville region is in an arid climate with hot dry summers and cold winters (Eggers, 2003). The Crooked River watershed averages 12 inches of rain per year, 90% of which falls between November and February. Winter temperatures often fall below 0°F (-18°C) (January average is 32 °F (0°C)), while summers rarely go above 100 °F (38°C) (July average is 60°F (15.5°C). The mean annual streamflow is approximately 270,000 acre-feet/year (1 acre-foot = 1233.5 m^3), ranging from 690,000 af/yr to 40,000 af/yr (Eggers, 2003).

The Crooked River watershed contains a variety of land cover types and diverse geography. It is bordered by mountain ranges on the northern and south-central boundaries. The southern region is comprised of mostly plains and grasslands (Gesch et al., 2002). The geology of the watershed includes basalt, fine grain volcanic duff and lava flows. Over time, erosion transformed the previously soft bed surrounding the reservoir to steep gullies. The reservoir is in a shallow valley surrounded by steep hillsides, 90% of which are highly erodible soils. Due to the highly erodible soils, the primary water quality concern for both the Crooked River and

Prineville reservoir is turbidity (Eggers, 2003). In addition to the erodible hillslopes, other erodible soils (i.e. montmorillonite clay) and upstream land use (logging, roads, heavy livestock grazing) add to the erosion and turbidity build up in Crooked River and Prineville reservoir. From 1960 to 1998, Prineville Reservoir lost nearly 5000 acre-ft of storage due to sedimentation.

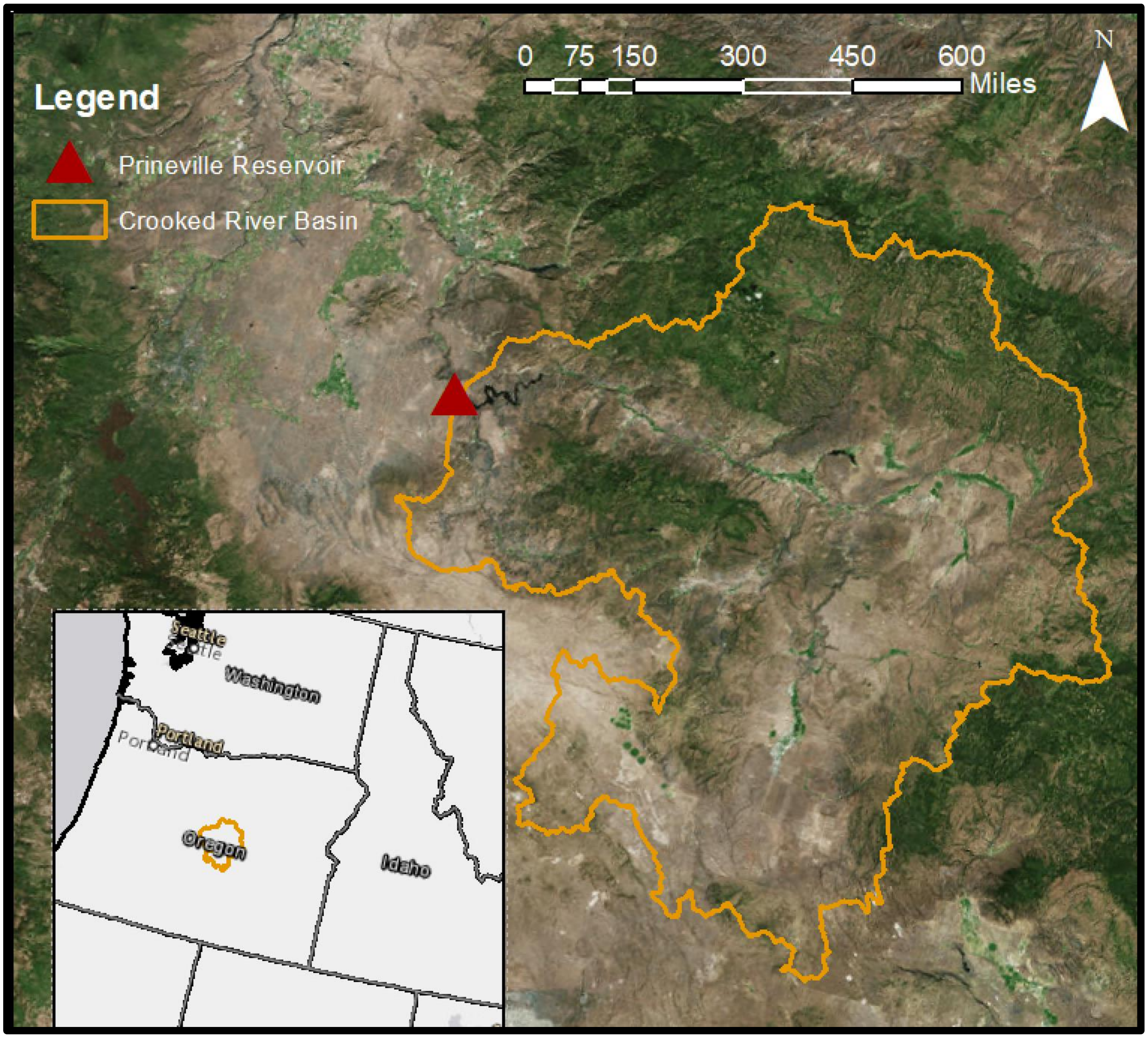

Figure 2.1: Map of the Cooked river watershed in central Oregon. The watershed is delineated by the orange line and the reservoir is located at the red triangle.

2.2 Data Sources

The data sources for this study are summarized in table 2.1. They include hydrometeorological data, soil and vegetation parameters, streamflow measurements and reservoir volume surveys.

The hydrometeorological data used as inputs for the VIC model were developed by (Livneh et al., 2015, 2013). The dataset provides daily maximum and minimum temperature, windspeed and precipitation values. It is gridded for the Conterminous United States (CONUS) on a 1/16° resolution. The soil texture values (more details on this will follow) are from survey data, although some will be varied for a sensitivity analysis (Mill and White, 1998). The inputs for VIC comprise of a variety of soil characteristics including infiltration, hydrologic conductivity and maximum baseflow velocity.

Daily average streamflow observations came from U.S. Geological Survey (USGS) gage 14080500, Crooked River near Prineville, OR. Streamflow data from the USGS are available from 1941 to 2018 and are not corrected for the influence of upstream reservoir intakes. The USGS data were supplemented by the USBR Hydromet (hydrologic and meteorological monitoring stations) historical dataset. In addition to streamflow, Hydromet includes naturalized streamflow for post-dam construction flows in addition to uncorrected discharge flows. The naturalized streamflow is reported as daily average flow starting in 1973 continuing to the present, and discharge flows are available from 1941 to 2018.

Reservoir volumetric surveys collected by USBR were used to quantify volume loss in Prineville Reservoir (Ferrari, 1999).There are two available surveys for Prineville collected in 1960 and 1998. The survey method used in 1998 was sonic depth recording interfaced with GPS giving continuous sounding throughout the reservoir. The method used in the 1960 survey was not specified, but it was likely the line and sinker method which was common at the time. Notably, the limitation to reservoir surveys is that sediment density is often unknown. Sediment density can range from 40-100 lb/ft^3 with it most commonly falling between 60 and 80 lb/ft^3. Since the sediment survey data for Prineville lacks a density measurement, the entire range of density is considered here.

Table 2.1: Data sources used for model inputs and model analysis

Data Type	Dates	Citation
Soil Parameters		(Maurer et al., 2002)
Vegetation Parameters		(Hansen et al., 2000)
Meteorology	1915 to 2015	(Livneh et al., 2015)
Streamflow	1941 to 2018	(U.S. Geological Survey, 2016)
Naturalized Flow	1973 to 2018	(U.S. Bureau of Reclamation, 2016)
Reservoir Volume	June 1, 1960 and May 31 1998	(U.S. Geological Survey Water Information Coordination Program, 2014)

2.3 Hydrologic Model and Sediment Algorithms

The sediment ensemble for this study was developed by Stewart et al., (2017). It consists of five algorithms, three of which are hydrologically forced. In this study, we will be using the three hydrologically forced algorithms which are outlined in the following sections. Important parameters for these algorithms are described further in table 2.2.

2.3.1 Hydrologic Model – Variable Infiltration Capacity model

The Variable Infiltration Capacity model (VIC) will be used to model hydrologic processes needed to drive the sediment algorithms (Liang et al., 1994). VIC is a widely used, distributed hydrologic model that uses soil, vegetation and meteorological forcing inputs to compute surface water and energy balances. For this application it is run on 1/16° (~ 6 km) grid cells at a daily time step. The processes important to sediment yield include precipitation impact, surface runoff and total streamflow.

Precipitation is the most influential driver of sediment development and transport. It is the mechanism for erosion via raindrop impact and contributes to runoff. Runoff transports sediment particles to streams. The quantity of erosion from precipitation and rate of transport from streamflow relies on the canopy and vegetation type which influence interception. Interception modulates raindrop impact by preventing drops from reaching the surface and forming larger drops on leaves that eventually reach the ground. The vegetation type and vegetation density also influence runoff magnitude by changing the interception rates. Surface runoff collects eroded soil from raindrop impact and carries it to streams which eventually deposit it into reservoirs. Along the way, the flow erodes streambanks creating more sediment while some sediment settles in the streambed.

Runoff is calculated as the excess precipitation after infiltration (the difference between precipitation and infiltration). In equation (2.1) for infiltration, i is the infiltration capacity, i_m is the maximum infiltration, A is the fraction of area in which the infiltration capacity is less than i and b_i is the infiltration shape parameter.

$$i = i_m[1 - (1 - A)]^{1/b_i} \tag{2.1}$$

Runoff can then be expressed as equation 3 where, Q_d is surface runoff, Q_b is subsurface flow both in units of millimeters, and $C_{v\,i}$ is the vegetation class.

$$Q = \sum_{i=1}^{N+1} C_{v\,i} * (Q_{d\,i} + Q_{b\,i}) \tag{2.2}$$

2.3.2 Sediment Ensemble

Three sediment algorithms will be evaluated in this study. Each algorithm was coupled with VIC internally by adding the algorithms to the source code. Within the source code, hydrologic variables such as precipitation, runoff and baseflow were applied explicitly to the algorithms.

Modified Universal Soil Loss Equation

The Modified Universal Soil Loss Equation (MUSLE) is an empirical algorithm that uses catchment characteristics to predict soil erosion based on the peak streamflow and total volume of an event (Arnold et al., 1998). The average soil loss (A) is calculated from equation 2.3.

$$A = RKLSCP \tag{2.3}$$

R is the runoff factor (see equation 2.4) which is calculated using the total runoff in an event (Q, mm) and peak streamflow rate of the event (q_p, mm). When imbedded into VIC, q_p was defined as the max streamflow rate during a 24-hour time step. *K* is the soil erodibility index, LS (m) is a topographical index for the length and steepness of the slope, C is a crop management factor for vegetation and P is a landcover factor.

$$R = 11.8(Q * q_p)^{0.56} \tag{2.4}$$

The MUSLE equation is limited by its assumption that the soil loss is linearly proportional to a set of catchment characteristics. In addition, because it is an empirical algorithm many of the inputs are not directly measured, hence they are difficult to determine.

Hydrological Simulation Program—Fortran

The Environmental Protection Agency (EPA) developed the Hydrological Simulation Program – Fortran (HSPF) based on the Stanford Watershed Model (Bicknell et al., 1996; Johanson et al., 1980). It is a conceptual algorithm that uses hillslope erosion algorithms for soil detachment from rainfall and scour by overland flow. These processes were embedded into the VIC framework. Rainfall detachment ($DET, \frac{tons}{ac}/interval$) considers the kinetic energy of raindrops as seen in equation 2.5. dt is the number of hours in the time interval, RC is the fraction of snow and vegetation cover, P is the practice management factor from USLE (the universal soil loss equation), K is the detachment coefficient from USLE, I ($\frac{in}{interval}$) is the rainfall intensity and JR is the detachment exponent.

$$DET = (dt(1 - RC)(P)(K)(\tfrac{I}{dt}))^{JR} \tag{2.5}$$

To estimate SSL, HPSF uses transport capacity (*TC*, *tons/ac/interval*) in equation 2.6 where *KS* is the transport coefficient, *SU* (*in*) is surface water storage, *SO* (*in/interval*) is surface water outflow and *JS* is the transport exponent. The transport capacity represents the amount and size of sediment that can be carried by the flow of water in a stream. The higher the flowrate, the higher the transport capacity. As the transport capacity decreases, particles are deposited on the streambed because settling velocity of some sediment particles is greater than the transport capacity.

$$TC = dt(KS)\left(\frac{SU+SO}{dt}\right)^{JS} \tag{2.6}$$

The effect of the previous day's rainfall on sediment production is simulated by decreasing DET for days without a storm event. This is done with the AFFIX parameter in equation 2.7 which increases each day due to soil compaction.

$$DET = DET(1.0 - AFFIX) \tag{2.7}$$

A feature of HSPF is that it is relatively simple, as it uses concepts of physical mechanisms to drive SSL generation. However, many of the coefficients and exponents are not directly measurable and rely on calibration to estimate values. In turn, calibration relies on observations. The nature of calibrating non-physically based parameters can lead to over fitting.

Systeme Hydrologique European Sediment Algorithm

The Systeme Hydrologique European Sediment algorithm (SHE-SED) (Wicks and Bathurst, 1996) is a sediment transport scheme used within the Distributed Hydrology Soil Vegetation Model (DHSVM) (Wigmosta et al., 1994). DHSVM is a physically based distributed model that solves the energy and water balance equations. SHE-SED is the most complex of the algorithms used in this study. DHSVM and SHE-SED rely on fine resolution vegetation and topography, which causes limitations on large scale modeling efforts. The hillslope erosion algorithms for overland flow and raindrop impact from the SHE-SED algorithm were embedded into the VIC framework. By removing the SHE-SED algorithms from DHSVM, the algorithm no longer includes the dynamic routing scheme DHSVM is known for which may influence its performance. Henceforth, this algorithm will be referred to as DHSVM.

Overland flow detachment (D_{of}, $m^3/s/m$) quantifies the sediment that is eroded by overland flow. It is calculated by equation 4 where β_{de} is the detachment coefficient, dy (m)is the horizontal hillslope length, $v_s(m/s)$ is the settling velocity, and TC (m^3/m^3) is the transport capacity.

$$D_{of} = \beta_{de}(dy)(v_s)(TC) \tag{2.8}$$

Raindrop detachment is the erosion from raindrop impact. It is calculated as the momentum squared of direct throughfall (M_R) and leaf drip from vegetation (M_d) from equations (2.9) and (2.10) respectively. I (*mm/hr*) *is* rainfall intensity, α and β are coefficients from (Wicks, 1988), V is leaf drip fall velocity, ρ $(kg/m^2/s)$ is water density, $D(m)$ is leaf drip diameter, $Drip$ is the percent of canopy drainage that falls from leaves and $Drain$ (m/s) is drainage from the canopy.

$$M_R = \alpha I^{\beta} \tag{2.9}$$

$$M_d = \frac{\left(\frac{V\rho\pi D^3}{6}\right)^2 Drip\ Drain}{\left(\frac{\pi D^3}{6}\right)} \qquad (2.10)$$

Critical Area Approach

Each model is applied on 1/16-degree VIC grid cells (~6 km). In large basins, (greater than 500km^2) 6 km grid cells provide an adequate resolution for modeling hydrology. However, many erosion processes occur on the scale of meters. The spatial discretization needed to quantify sedimentation is limited by computational power and available data at the scale of 6 km. Instead, the critical area approach is used to quantify sediment development on individual hillslopes that can then be upscaled to the larger VIC grid cells.

Critical areas are defined as the portion of the model grid cell that contributes to the suspended sediment load, which is used to determine where soil erosion is most likely to occur. In Stewart et al., (2017), critical areas were determined by using a threshold of slope steepness and stream proximity. In this study, the critical area was included in the sensitivity analysis with a range of values from 0 % to 100 % to determine the importance of estimating the critical area accurately for reservoir sedimentation estimates.

Modeling Assumptions for Reservoir Sedimentation

Stewart et al., (2017), developed the sediment ensemble to include a routing scheme. However, for the application to reservoir sedimentation, the timing of SSL is less important than other applications, since we are primarily interested in sediment accumulation on longer timescales (monthly to decadal) rather than the shorter timescales (hourly to daily) relevant to water treatment. For this reason, the sediment routing scheme was not included in the present application of the model ensemble. It is important to note that because sediment routing is not included, the results presented here are only applicable to long-term (monthly to decadal) sedimentation.

The second major assumption in comparing accumulated SSL with surveyed reservoir sediment is that SSL comprises all loading into the reservoir. This assumption precludes sediment from bedload which can be up to 10% of the total sediment yield. Therefore, for drainages with large bedload this assumption will not be valid.

2.4 Sobol Sensitivity Analysis

The reservoir sedimentation estimates in this thesis are a new application of the multi-algorithm sediment ensemble method developed by J. Stewart et al. (2017). To evaluate this new application and to understand key sensitivities in modeling reservoir sedimentation, a Sobol Sensitivity Analysis is performed, herein "Sobol", (Sobol, 2001). Sensitivity analyses assist modelers in identifying the importance of parameters for a desired output. The sensitivity analysis for streamflow and sediment will be done independently. Stewart et al. (2017) performed a joint calibration—a simultaneous calibration of both streamflow and sediment parameters—but did not perform a sensitivity analysis. The best performing simulation from the streamflow sensitivity analysis will be used to force the sediment ensemble. By isolating the sensitivity analysis for the streamflow model from the sediment ensemble, it ensures the streamflow inputs are as realistic as possible when used to drive the sediment ensemble. This is important because sediment accumulation relies heavily on streamflow magnitude.

2.4.1 Theory

Sobol is a variance-based global sensitivity analysis which allows sampling of the entire range of input parameters (Sobol, 2001). Sobol uses an ensemble of parameter realizations to evaluate parameter influence on the variance. This study uses the *Saltelli* improvement of Sobol which increases the efficiency by decreasing the number of parameter sets needed in the model ensemble (Saltelli, 2002). From the variation in the ensemble of model outputs, Sobol produces indices that that identify the fraction of the variance of the output that is influenced by a given parameter or set of parameters and represent parameter sensitivity. The outputs used here are a set of objective functions used to describe the skill of the streamflow model and sediment algorithm outputs, relative to observations.

Sobol indices are based on variance decomposition which attributes the total variance to specific parameters and parameter interactions. The decomposition of the variance is detailed in equation 2.11.

$$V(Y) = \sum_{i=1}^{k} V_i + \sum_{i<j} Vij \ + \cdots \ V_{1\ldots.k} \qquad (2.11)$$

k is the number of varied parameters, *i* and *j* identify parameters from the set of varied parameters and *V* is the variance of a given set of parameters which are identified by the subscripts.

Sobol sensitivity indices range from 0 to 1 where 1 signifies parameters that are most sensitive. Sensitivity indices are based on the parameter's contributions to *V(Y*). Equation 2.12 represents the calculation for a Sobol total sensitivity index for a single parameter *i* where S_{Ti} is the total sensitivity, *V* is the variance of the model and V_i is the variance of parameter *i*.

$$S_{Ti} = \frac{V_i}{V} + \sum_{j \neq i} \frac{V_{ij}}{V} + \cdots + \frac{V_{ij\ldots k}}{V} \qquad (2.12)$$

The first order sensitivity index ($S_{1st,i}$) is the first term of the total order sensitivity index calculation. The interaction term is the sum of the remaining terms. The interaction sensitivity is calculated with equation 2.13.

$$S_{Ni} = S_{Ti} - S_{1st,i} \qquad (2.13)$$

Typically, three sensitivity indices are used to evaluate a model: First order, total order and interaction sensitivity indices. Consider a model that has output Z and inputs X and Y. The variance of Z can be decomposed into the variance caused by changes in X (first order sensitivity), the variance caused by changes in Y (first order sensitivity) and the variance caused by the interaction between X and Y (interaction sensitivity). The total order variance of X is the sum of the variance caused by changes in X and the variance caused by X when Y is also varied. The total order variance of Y is the sum of the variance caused by changes in Y and the variance caused by Y when X is also varied. With more than two parameters, the interaction variance can be decomposed into second order, third order, fourth order, and so forth. For example, second order variance is the variance caused by one parameter when two others are also varied.

Sobol uses a quasi-random sampling method similar to Latin hypercube sampling called a Sobol sequence (Sobol, 1976). The Sobol sequence ensures that the global parameter space of each parameter is evenly distributed. It does this by adding samples to the parameter space away from previously established samples (Nossent et al., 2011). The samples produced from this technique will be used to perform the Sobol sensitivity analysis.

2.4.2 Application

In simple models, the sensitivity of all parameters can be calculated. However, due to the complex and computationally intensive nature of VIC and sediment ensemble, a subset of parameters was selected to adhere to computational restraints. The parameters in table 2.2 were chosen for the sensitivity analysis based on Stewart et al. (2017).

The number of model realizations depends on the number of parameters and the desired sample size. For complex environmental models, sample sizes range between 1000 and 2000 (Houle et al., 2017; Nossent and Bauwens, 2012; Tang et al., 2007; van Werkhoven et al., 2008;

Zadeh, 2015). For this study a sample size of 2000 is used to ensure adequate sampling of each parameter range. The number of model runs is calculated by equation 2.14 (Saltelli, 2002).

$$N = n(2K + 2) \tag{2.14}$$

Table 2.2. Parameter selection for VIC and sediment sensible algorithms used in the Sobol sensitivity analysis including definitions and ranges.

Parameter	**Definition and Relevant Models**	**Lower Limit**	**Upper Limit**
Binf	Infiltration Capacity (VIC)	0.0001	0.4
Ds	Fraction of DsMax where non-linear baseflow occurs (VIC)	0.001	1
DsMax	Maximum baseflow velocity (VIC)	0.1	30
Ws	Fraction of maximum soil moisture where non-linear baseflow occurs (VIC)	0.1	1
C	Baseflow curve exponent (VIC)	1	2
Layer 2	Soil layer depth 2 (VIC)	0.3	4
Layer 3	Soil layer depth 3 (VIC)	0.3	4
Snow Roughness	Surface roughness of snowpack (VIC)	0.0001	0.05
K Factor	Erodibility factor (MUSLE, HSPF)	0.2	0.6
C factor	Cropping management factor (MUSLE, HSPF)	0.001	0.5
P factor	Conservation management factor (MUSLE)	0	1
K Index	Conservation practice factor (DHSVM)	19	32
D50	Median grainsize (DHSVM)	0.5	2
B_{de}	Soil cohesion (DHSVM)	0.00075	15
JR	Detachment exponent (HSPF)	1	3
AFFIX	Attachment fraction (HSPF)	0.01	0.5
KS	Transport coefficient (HSPF)	0.1	0.5
JS	Transport exponent (HSPF)	1	3
KG	Scour coefficient (HSPF)	0	10
JG	Scour exponent (HSPF)	1	5
Critical Area	Catchment critical area (MUSLE, HSPF, DHSVM)	0.002	0.04

K is the number of parameters, n is sample size and N is the total number of model runs. The sensitivity analysis for stream flow includes 8 parameters resulting in 36,000 parameter realizations. The analysis for sediment includes 13 parameters, thus resulting in 60,000 realizations.

2.5 Model Performance Measures

The streamflow model and sediment ensemble sensitivities are evaluated using objective functions. Selecting appropriate objective functions is important because each objective function emphasizes specific aspects of the behavior of the model (McCuen et al., 2006). They were selected from common hydrologic objective functions that address aspects important for sediment estimates. They are detailed in equations 2.15 to 2.21. For the following equations S is the simulation, O is the observation, N is the number of observations and i corresponds to an observation or simulation at a specific moment in time. The objective functions used here are NSE for overall fit, RMSE for overall error, R for timing errors, ratio of the variance for variability and percent bias for systematic biases.

In a subsequent analysis, RMSE was also used to evaluate the extent to which the sediment algorithms predict sediment accumulation that differs from the traditional linear assumption. Finally, the amount of sediment accumulation from the first half of the model simulation to the second half of each model simulation was compared with a percent difference.

Nash Sutcliffe Efficiency

The Nash Sutcliffe Efficiency (NSE; Nash and Sutcliffe, 1970) was developed for specific use in hydrology and has become a commonly used objective function in the field (Gupta et al., 2009). The calculation, provided in equation 2.15, includes components of correlation, bias and variability. NSE values range from -∞ to 1, with 1 being a perfect match and 0 being that the simulations do an equivalent job of matching the observations as the mean of the observations.

$$NSE = 1 - \frac{\sum_{i=1}^{N}(S_i - O_i)^2}{\sum_{i=1}^{N}(O_i - \overline{O})^2} \tag{2.15}$$

NSE is sensitive to a number of factors, including sample size, outliers, magnitude bias, and time-offset bias (McCuen et al., 2006). One of the main concerns about NSE is its use of the observed mean as baseline, which can lead to overestimation of model skill for seasonally driven variables such as runoff in snowmelt dominated basins (Gupta and Kling, 2011).

Pearson Correlation Coefficient

The Pearson correlation coefficient (R) helps determine if a positive or negative linear relationship is present. It ranges from -1 to 1, with 1 being an exact positive relationship and -1 being an exact negative relationship. One drawback to the R metric is that it only measures linear relationships and can be easily skewed by outliers. R is calculated by equation 2. 16.

$$R = \frac{\sum_{i=1}^{N}(S_i - \overline{S})(O_i - \overline{O})}{\sqrt{\sum_{i=1}^{N}(S_i - \overline{S})^2 \sum_{i=1}^{N}(O_i - \overline{O})^2}} \tag{2. 16 }$$

Ratio of Variances

The ratio of variances is a comparison between the variance of modeled and observed data. It ranges from 0 to ∞ with an optimal value of 1 signifying the variances are equal. Values near 1 indicate high model skill. In terms of streamflow, a value near one would tell us that the model and observations agree on extreme low and high flows. A value near zero indicates the model has high peak and the observations have low peaks where as a value near infinity would indicate the opposite. The variance is shown in equation 2.17 and the ratio of the variances in equation 2.18 .

$$\sigma^2 = \frac{\sum_{i=1}^{N}(X_i - \overline{X})^2}{N} \tag{2.17}$$

$$Variance\ ratio = \frac{\sigma_s^2}{\sigma_o^2} \tag{2.18}$$

Percent Bias (PBIAS)

Percent bias is a measure of systemic error. It measures the degree which the model provides values above or below observed (Maidment, 1993). More simply, percent bias is the difference in the accumulation of the model output and observations. Theoretically, values can range from -∞ to ∞ with an optimal value of 0%. Negative values are underestimations and positive values are over estimations. Percent bias is calculated with equation 2.20.

$$PBIAS = 100\ \frac{\sum_{i=1}^{N}(S_i - O_i)}{\sum_{i=1}^{N} O_i} \tag{2.19}$$

Percent bias is helpful in hydrology because it can determine the quantitative difference in the modeled values and observed values over extended time periods (Boyle et al., 2000). It is applicable for reservoir sedimentation because accuracy over many years (5-20 or more) is especially important for reservoir management.

Root Mean Squared Error

Root mean squared error (RMSE) is the standard deviation of the residuals for a predicted value (modeled) and a known value (observed). Smaller values signal better model performance with zero being perfect. There is no upper limit to the value of RMSE. RMSE is calculated with equation 2.20.

$$RMSE = \sqrt{\frac{1}{N}\sum_{i=1}^{N}(S_i - O_i)^2} \tag{2.20}$$

2.6 Sediment Yield Linearity

A major goal of this research is to assess the validity of assuming linear sediment yield. To this end, we chose a set of “behavioral” simulations that provide probable estimates of sedimentation. Although there exist two sediment volume surveys for Prineville Reservoir, the sediment density is unknown. Therefore, instead of having a single known value of volume loss, we have a range of possible sediment volume loss, governed by the sediment density range of 40 -100 lb/ft^3, which is the full range of sediment densities. In future studies a narrower sediment density range could be used. We use this information to choose behavioral simulations, defined as the set of model realizations that have their final accumulated sediment volumes falling within the density range.

To evaluate the relative yield linearity of each sediment algorithm we employ an RMSE calculation that can be considered the “Root Mean Squared Difference” between modeled sediment yield and the simple linear yield assumption of constant accumulation through time. Because the root mean squared difference equation is functionally equivalent to the classic RMSE equation, the term RMSE will be used, although the values are not considered “errors” necessarily since the exact sediment density is unknown. Specifically, the RMSE will be calculated for *yearly* sediment accumulation between the modeled yearly accumulation and the linear assumption accumulation. Then the reported RMSE is the difference in the yearly average between the sediment algorithm and the linear yield assumption. Moreover, the RMSE values will also be expressed as a percentage difference, showing how the accumulated differences between modeled sedimentation compares to the linear sedimentation estimates. The percent difference will simply be the yearly RMSE for a given model divided by the linear yearly sediment accumulation for a given simulation realization.

A final consideration in this analysis is how to calculate the assumed linear yield rate. Broadly, the yield linearity assumption is essentially a monotonic accumulation beginning at zero on the day of the first reservoir survey and ending at the value of modeled sediment accumulation on the day of the final reservoir survey. Thus, the linear yield estimate is dependent on the final sedimentation accumulation, which is not strictly known. Rather than compare simulated sediment accumulation to a single linear function, which would assume a known sediment density, each simulation is compared to a different linear yield rate equation based on the final modeled sediment accumulation value.

The second method used to determine yield linearity is a comparison of sediment accumulation between two time periods. The simulation spans 1960 to 1998 which will be split into time period 1 (1960 to 1979) and time period 2 (1979 to 1998). The accumulated sediment for these 19-year spans will be compared with a percent difference for each simulation.

Chapter 3: Results

Overview

The results are discussed in the following three sub-sections. First, the sensitivity analysis and parameter selection for streamflow are presented. This is followed by the sensitivity analysis and parameter investigation for the sediment ensemble. For each analysis, the sediment ensemble results are presented in the following order: MUSLE, HSPF, DHSM. Finally, there is an evaluation of the yield linearity of each sediment algorithm.

3.1 Streamflow Sensitivity

The sensitivity analysis for VIC streamflow was performed on modeled streamflow from 1975 to 1998 to match the available naturalized flow data after reservoir construction. Figure 3.1 shows the results of the sensitivity analysis. Sobol sensitivity indices range from 0 (white) indicating no sensitivity, to 1 (dark purple) with 1 indicating the most sensitivity. Each square in the matrix represents the sensitivity of a parameter for a single objective function.

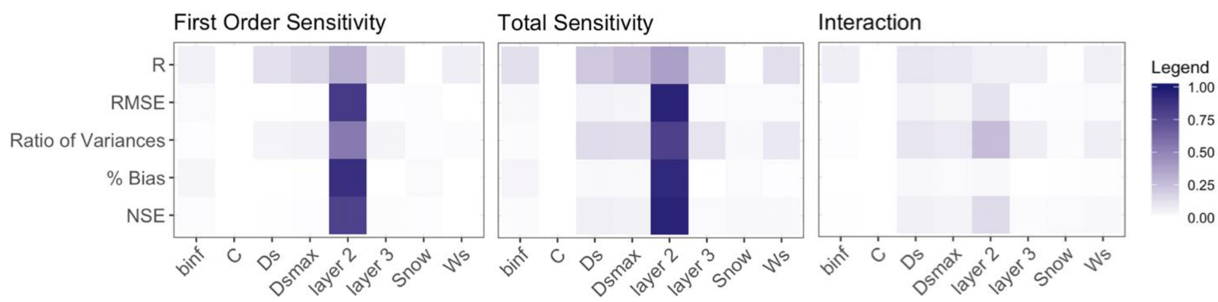

Figure 3.1: First order sensitivity, second order sensitivity and interaction for streamflow objective function from VIC. Dark colors represents more sensitive parameters.

Demaria et al., (2007) used a Monte Carlo sensitivity analysis to find that layer 2 and binf were sensitive parameters for VIC streamflow. There is broad agreement that streamflow is sensitive to changes in layer 2 with a strong first order sensitivity. However, in contrast to Demaria et al. (2007) binf—the infiltration capacity of the soil—appears to be insensitive in this analysis. The streamflow's minimal sensitivity to binf can be explained by the Crooked River watershed's arid climate, with only 11 inches of precipitation per year. For the Crooked River watershed, infiltration is controlled by the amount of runoff. Even if there is a high infiltration capacity, there is a limit to the amount of runoff available to infiltrate into the soil. Based on the VIC model simulations, the Crooked River is assumed to be driven primarily by baseflow. This assumption comes from the model runoff to baseflow ratio from 1960 to 1998 (years of sediment volume surveys) is 0.38, showing that there is more than twice the volume of baseflow than runoff, as illustrated in figure 3.2b. Figure 3.2a shows that the yearly modeled accumulated streamflow and peak snow pack are similar values in most years, so the majority of streamflow develops as snowmelt, not runoff from precipitation.

Interaction sensitivity is the product of the variance produced by changing two or more parameters simultaneously. The sensitivity analysis for VIC shows little interaction sensitivity relative to first order sensitivity for layer 2. Ds and Ds_{max} show more interaction sensitivity compared to first order sensitivity for the ratio of variances, RMSE, percent bias and NSE. However, they show less sensitivity in correlation, R. R and Ratio of Variances have more sensitivity to parameter interaction than RMSE, percent bias and NSE.

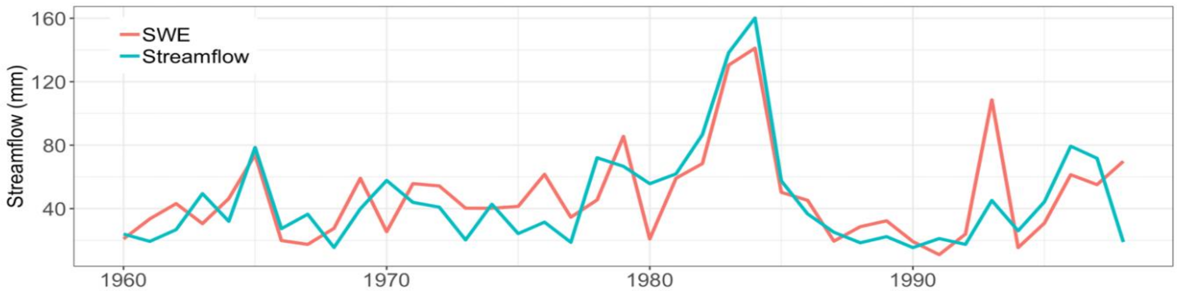

a)

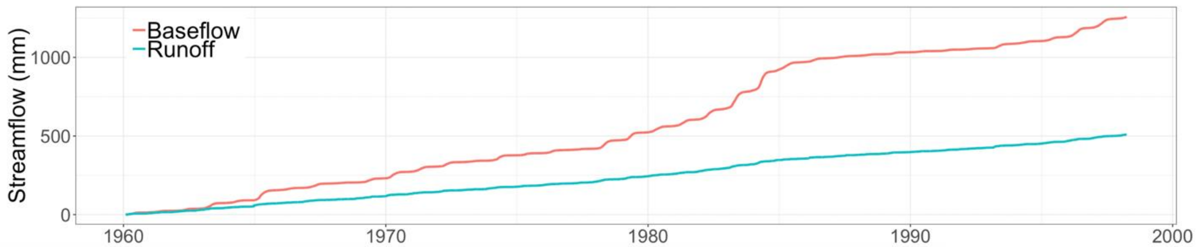

b)

Figure 3.2: a) Yearly maximum snowpack (SWE) and yearly accumulative streamflow (runoff and baseflow) from 1960 to 1998. b) Runoff and baseflow accumulation from date of the first reservoir volume survey to the date of the final reservoir volume survey. Data for both panels come from VIC simulations.

3.2 Streamflow Model Selection

The streamflow parameters that would be used to drive VIC were selected from the model instances used for the Sobol sensitivity analysis. The initial results from the model realizations used in the Sobol sensitivity analysis revealed discrepancies between the modeled and the observed streamflow. Typically, an NSE greater than 0.5 is desirable for streamflow. However, past studies found the Crooked River watershed challenging to model. Mendoza et al., (2017) found a best NSE of 0.34 for fully calibrated SAC- SMA (Sacramento Soil Moisture Accounting) model. A USBR study also found poor model performance for the Crooked River Basin (Turner, 2011). They used VIC and found a maximum R^2 value of 0.3. The primary concern for this study, where sediment is being mobilized, is that the peak flow magnitude and timing should match. An example is seen in figure 3.3, where the model struggles to produce these features, which is consistent with the aforementioned past studies.

A key modification was explored to improve the model result, namely the snow albedo parameters were adjusted because snowmelt is a key factor driving peak flow timing and magnitude. Notably, this modification occurred outside the usual set of soil parameters that are adjusted during calibration, i.e. this is a 'hard-coded' parameter. We following the guidance of past studies that highlighted the importance of modifying hard-coded parameters (Houle et al., 2017; Mendoza et al., 2017). The second round of Sobol simulations, resulted in much improved streamflow, shown in Figure *3.3.* below. The best results had an NSE around 0.28 and a R less than 10%, which are comparable to those by Mendoza et al. (2017) and Turner et al. (2011).

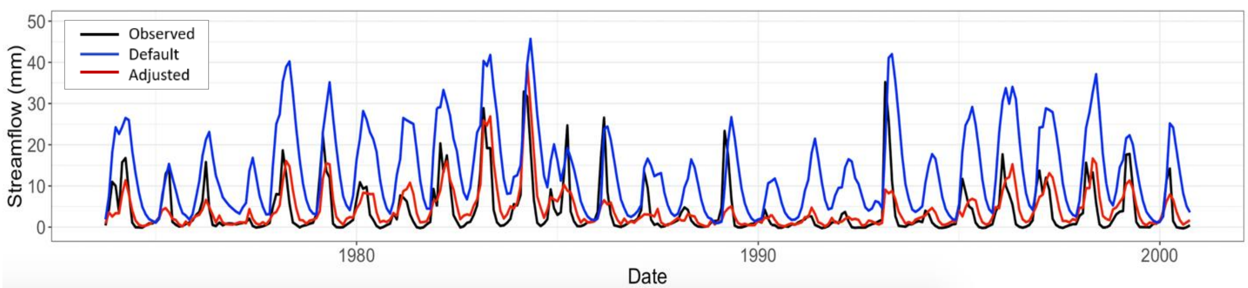

Figure 3.3: Monthly observed and modeled streamflow. The black line is the naturalized observed flow and the colored lines are model realizations. The blue line shows the model streamflow from the default albedo parameters. The red line shows the model streamflow from adjusted albedo parameters.

Table 3.1:a) Objective functions for the top performing streamflow parameters b)Parameters used to drive streamflow for the sediment ensemble

a)

NSE	% Bias	Var/Var	R
0.282	6.8	0.408	0.541

b)

Binf	Ds	Ds max	Ws	C	Layer 2 Depth	Layer 3 Depth	Snow roughness
0.0948	0.0040	10.93	0.910	1.44	0.997	3.59	0.043

The Sobol sensitivity analysis produced 40,000 model realizations of VIC streamflow. This number of realizations, together with comparable performance with past studies, gave us confidence that we had sufficiently sampled model space to select a set of streamflow parameters that would force the sediment ensemble as realistically as possible. The selected model realization had a percent bias of 6.8 and an NSE of 0.28 (see table 3.1a for all objective functions). Despite the low NSE, visual inspection shows that the model captures key features of the hydrograph reasonably well. The obvious issue is that the model severely underestimates peaks in 1985, 1986, 1989 and 1993. However, for other years the model matched the peak streamflow magnitude and timing to a satisfactory level. The selected parameters are in table 3.1b.

The assumption for the following sediment results is that VIC realistically models streamflow. First, the assumption is that VIC correctly partitions the total streamflow between baseflow and runoff. This is especially important because the sediment algorithms rely, to varying degrees, on the quantity of baseflow. The biases in the simulations of the VIC model variables, specifically runoff and baseflow will carry through the modeling process and impact sediment yield since the yield computation is driven by these hydrologic variables. The second assumption is that the soil and vegetation parameters did not change over time, i.e. static vegetation and soil parameter were used and would not account for alterations from development, agriculture, soil compaction, etc.

3.3 Reservoir Sediment Accumulation

The streamflow parameters selected through the model realizations used for the Sobol sensitivity analysis were used to drive the sediment ensemble. Sediment results are presented assuming that 100% of the sediment yielded by each algorithm will accumulate as reservoir sediment, e.g. a 100% trap efficiency. The model results, in kg, are compared to reservoir volume surveys measured in acre-feet. To convert the model output and observations to common units an assumption of sediment density was needed. Sediment density can range from 40-100 lb/ft^3. Range from the maximum to minimum sediment weight will be referred to as the sediment density error bars. The subset of model realizations with total accumulated sediment that falls within the sediment density error bars are considered ‘behavioral samples’ that are used to analyze the algorithms predicted reservoir sediment accumulation and sensitivity patterns. Figure 3.4 shows the behavioral subsets for each algorithm in the sediment ensemble. All three algorithms are driven partially by precipitation; the models differ in how they consider baseflow and runoff in the sedimentation equations.

The results for MUSLE are seen in figure 3.4a. MUSLE is an empirical algorithm that uses catchment characteristics and peak streamflow to determine sedimentation. Unlike the other algorithms that rely exclusively on surface runoff, MUSLE is driven by total streamflow (baseflow and runoff). The reservoir sediment accumulation pattern is driven by seasonal oscillations in baseflow because the watershed is baseflow dominant. The yearly jumps signal the algorithm’s ability to capture the seasonal oscillation in reservoir sediment accumulation. Baseflow accumulation is depicted in figure 3.2. In addition, there are changes in yearly reservoir sediment accumulations signified by the changes in slope between 1978 and 1985.

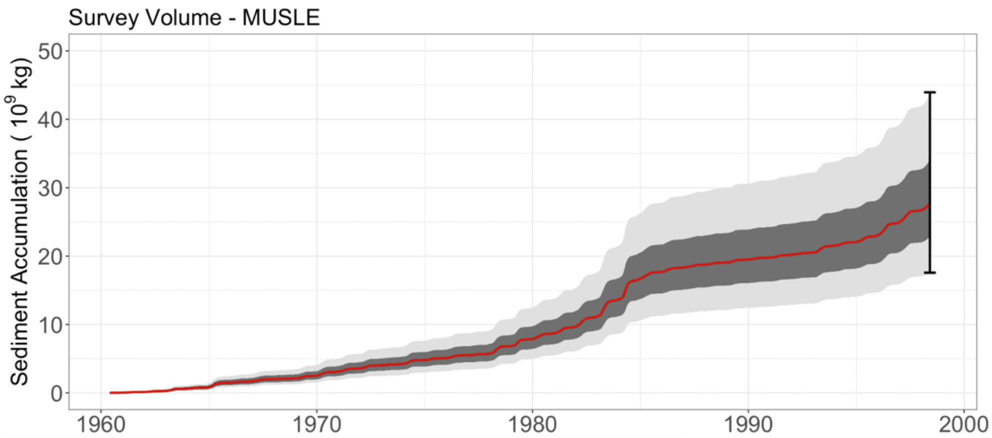

a)

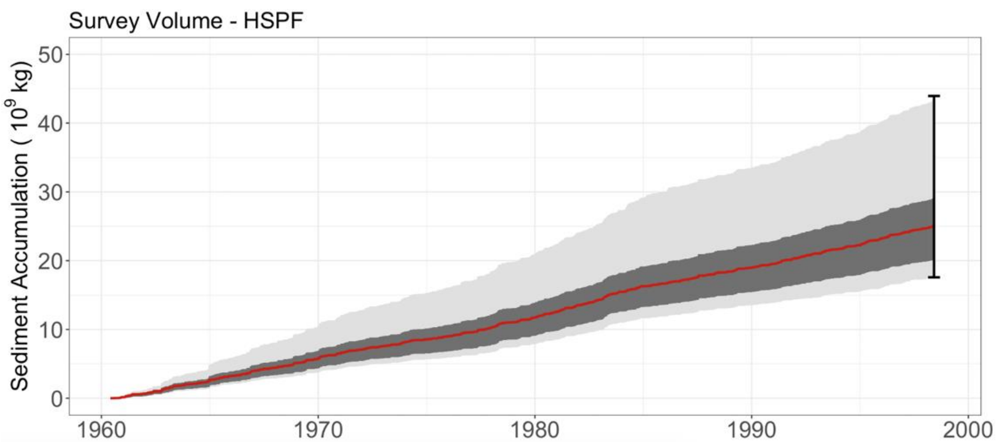

b)

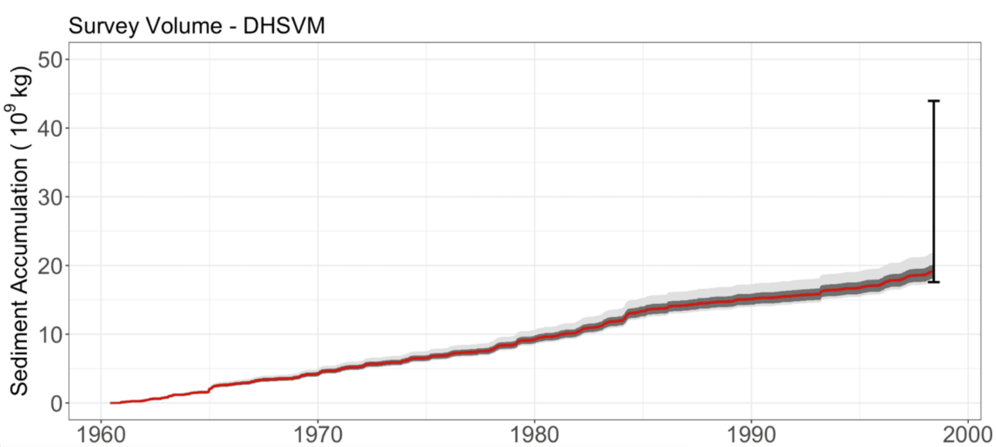

c)

Figure 3.4: Time series plot of accumulated reservoir sediment. A subset of behavioral algorithm realizations is shown for those that fall within the expected range of reservoir sediment accumulation based on the expected density range. The error bars are from the uncertainty in the sediment density. Red is the median, dark grey is the quartiles and light grey is other simulations that fall within the density error bars. MUSLE has 226 simulations that fall within the error bars, HSPF has 640 and DHSVM has 493. The simulations that have total reservoir sediment accumulation that fall outside of the error bars are not shown.

The results for HSPF are seen in figure 3.4b. HSPF is a runoff driven algorithm that solves the energy and water balance equation to calculate sedimentation. The similarities between HSPF and runoff can be seen in comparison to figure 3.4b and 3.2

The results for DHSVM are in figure 3.4c. There is some seasonal variation, but less than in MUSLE. The DHSVM realizations from Sobol, under estimate the reservoir sediment accumulation by a minimum of 30%. This poor performance is potentially because DHSVM was originally developed for hydrologic modeling in forested mountain regions, and the Crooked river basin is mostly flat grasslands. Furthermore, the DHSVM sediment physics are typically coupled with dynamic routing, which was not included here. A more holistic analysis into model physics would be required to address this issue in greater detail.

3.4 Sediment Sensitivity Analysis

To learn more about the processes behind the sediment development in each algorithm, we turn to a Sobol sensitivity analysis. Each algorithm relies on different parameters, so each algorithm has a different number of commonly calibrated parameters. Parameters chosen for the sensitivity analysis were selected from Stewart et al., (2017) resulting in nine parameters for HSPF, four for DHSVM and four for MUSLE[1]. The sensitivity analyses are presented in bar graphs in figure 3.5. In addition to the sensitivity analysis results, dotty plots and parameter distribution histograms are presented. The dotty plots show the relationship between the objective function (percent bias) used for algorithm evaluation and parameter changes.

[1] The results for MUSLE are not included because there were numerical errors in some model realizations, so the sensitivity analysis was not completed.

HSPF is more sensitive to parameter interactions than individual parameter changes. JG has the most first order sensitivity, but it is still less than its interaction sensitivity. JG and critical area have a high interaction index as well as JG and KG.

Figure 3.5: Bar graphs of Sobol sensitivity index values for DHSVM and HSPF. A value of one signals most sensitive, and zero signals no sensitivity.

DHSVM has high first order sensitivity of D50 and critical area. In addition, both parameters have a small amount of interaction sensitivity. Critical area is the percent of the area that contributes sediment to the outflow. The fraction ranges from 0% to 100%, with typical values falling between 30% and 100%. It is applied as a multiplier of the final sediment amount, so the results from the algorithm rely heavily on critical area.

3.5 Dotty Plots

Dotty plots are useful to see patterns in parameter sensitivities when comparing objective function for a range of parameter values (Wagener and Kollat, 2007). For example, they can be used to diagnose the behavioral ranges of a parameter, relative to a given objective function. In figure 3.6 and 3.7 the objective functions are on the vertical axis and the parameters are on the horizontal axis. When a dotty plot shows a relatively uniform distribution of points with respect to the vertical axis, this can be interpreted as little-to-no model sensitivity of the objective function to the given parameter. When a pattern emerges, the objective function is sensitive to changes in the parameter.

The dotty plots for HSPF are shown in figure 3.6. There is a similar exponential pattern for JS and JR parameters suggesting high algorithm sensitivity. JS and JR are scour and detachment exponents respectively. It is their application as an exponent that is seen in the dotty plot. There is also a slight exponential pattern in JG. The patterns exhibited on the dotty plots for the other parameters suggests a low amount of sensitivity. This agrees with the Sobol Sensitivity analysis.

The dotty plots for DHSVM are seen in figure 3.7. None of the simulations had percent bias below 30%. Critical area shows a distinct cutoff of objective function performance compared to the value of critical area. This is an expected pattern because the critical area is the percent of the catchment that is considered to contribute to sedimentation. As the critical area decreases the minimum percent bias will move farther from zero. The sensitivity would not be as strong if DHSVM generally underestimates sedimentation. The dotty plot for D50 (median grainsizes) shows the sensitivity in the form of algorithm performance cutoff as well. The cutoff here manifests from the grainsize because the grainsize influences the overland flow transport capacity.

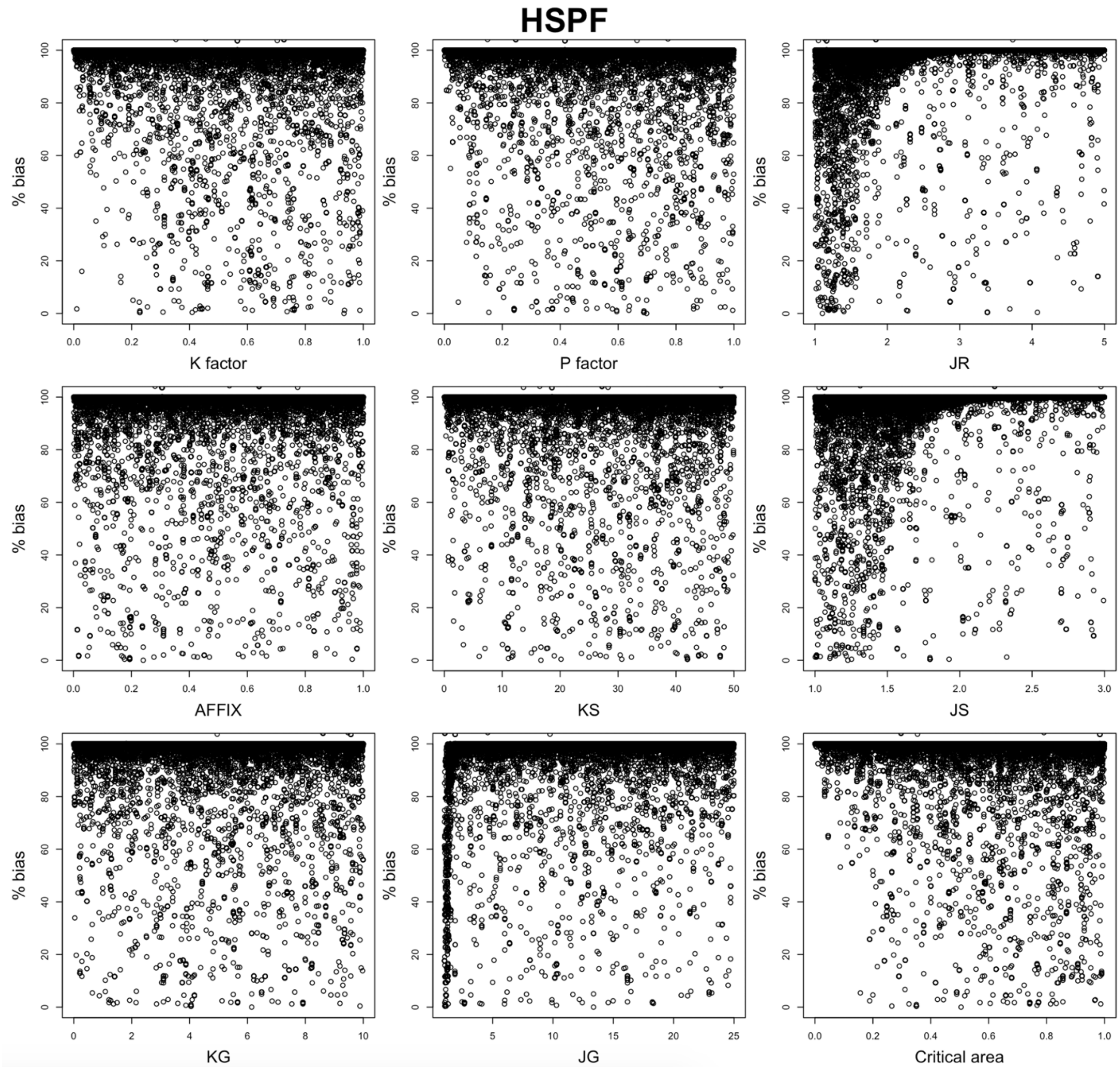

Figure 3.6: Dotty plots for HSPF algorithm realization with the absolute value of the absolute percent bias on the y axis and the parameter value on the x axis.

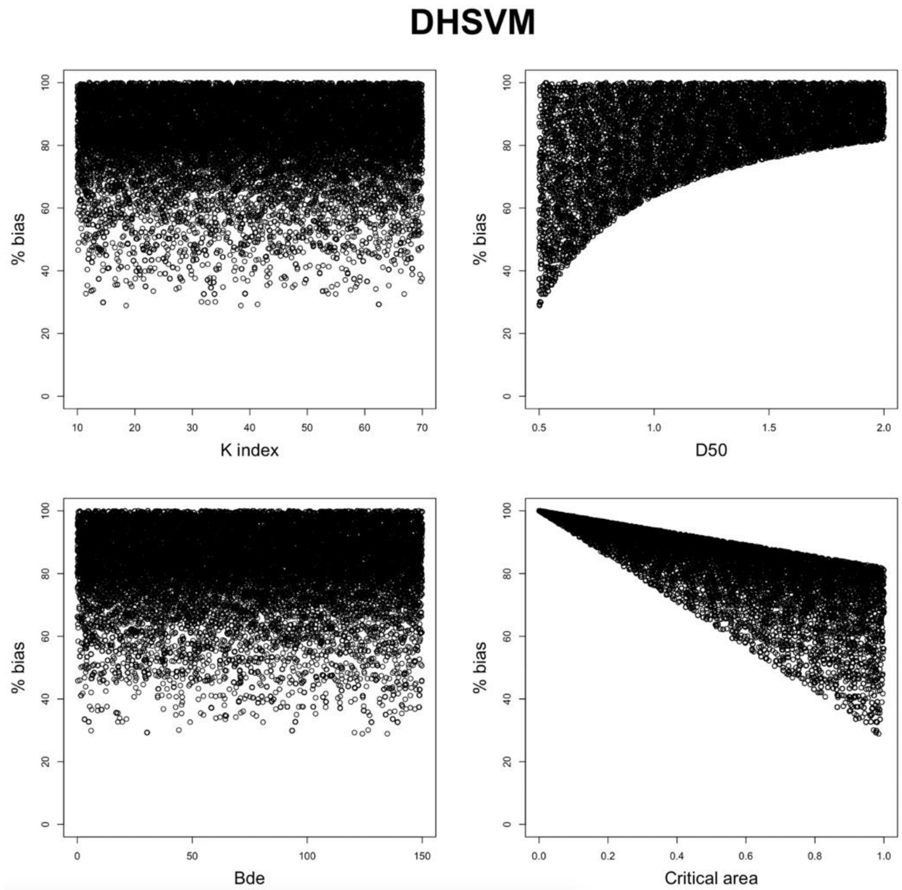

Figure 3.7: Dotty plots for DHSVM algorithm realization with percent bias on the y axis and the parameter value on the x axis.

Figures 3.8 and 3.9 are histograms of the parameter values for behavioral sediment simulations that fall within the sediment density boundaries. The values for each parameter in most cases span the entire range of possible inputs. The histogram shows which parameter values are most common within the subset of simulations that fall within the sediment density boundaries.

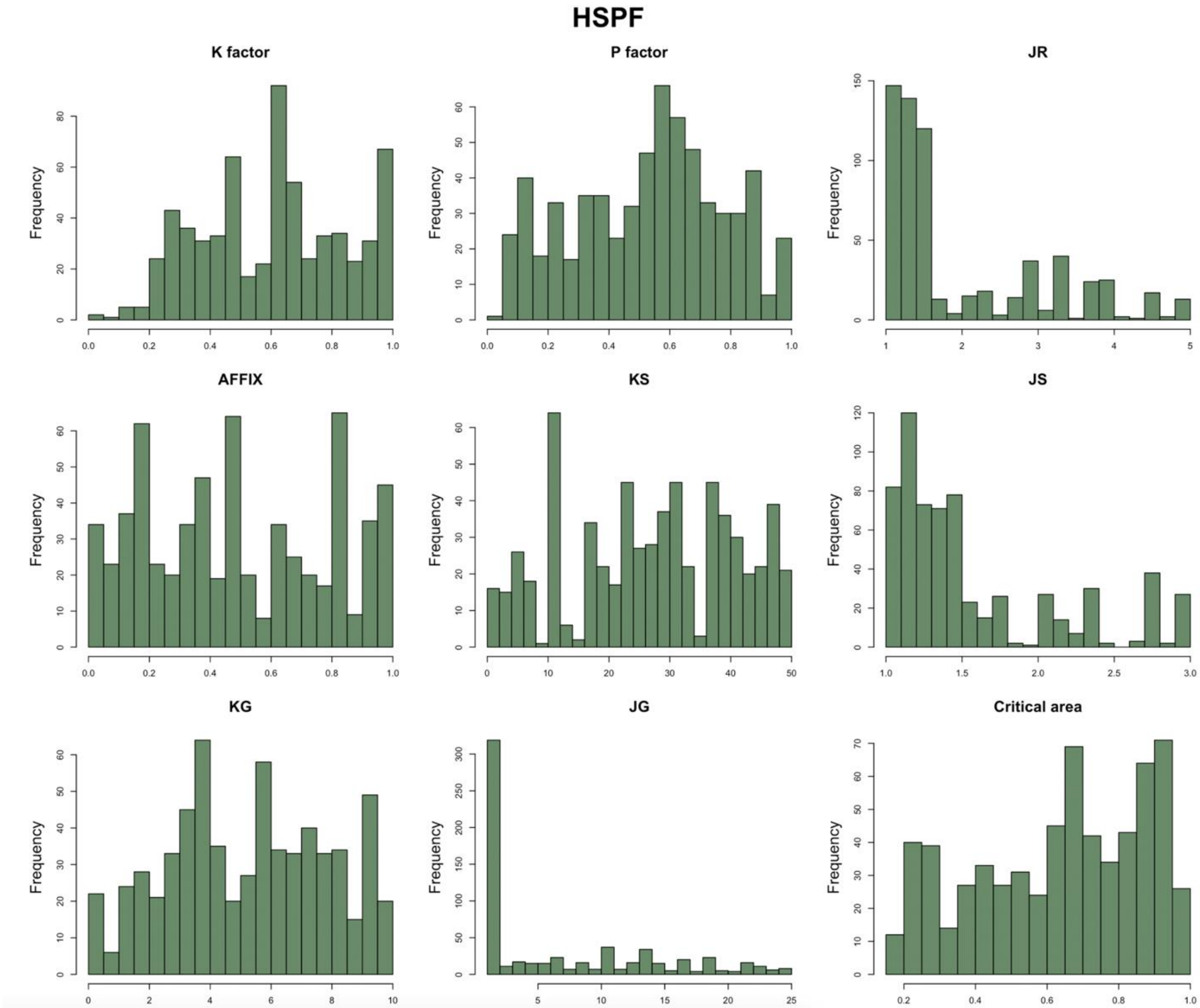

Figure 3.8: Histograms of the parameter distributions for behavioral algorithm realizations that fall with in density error bars for HSPF.

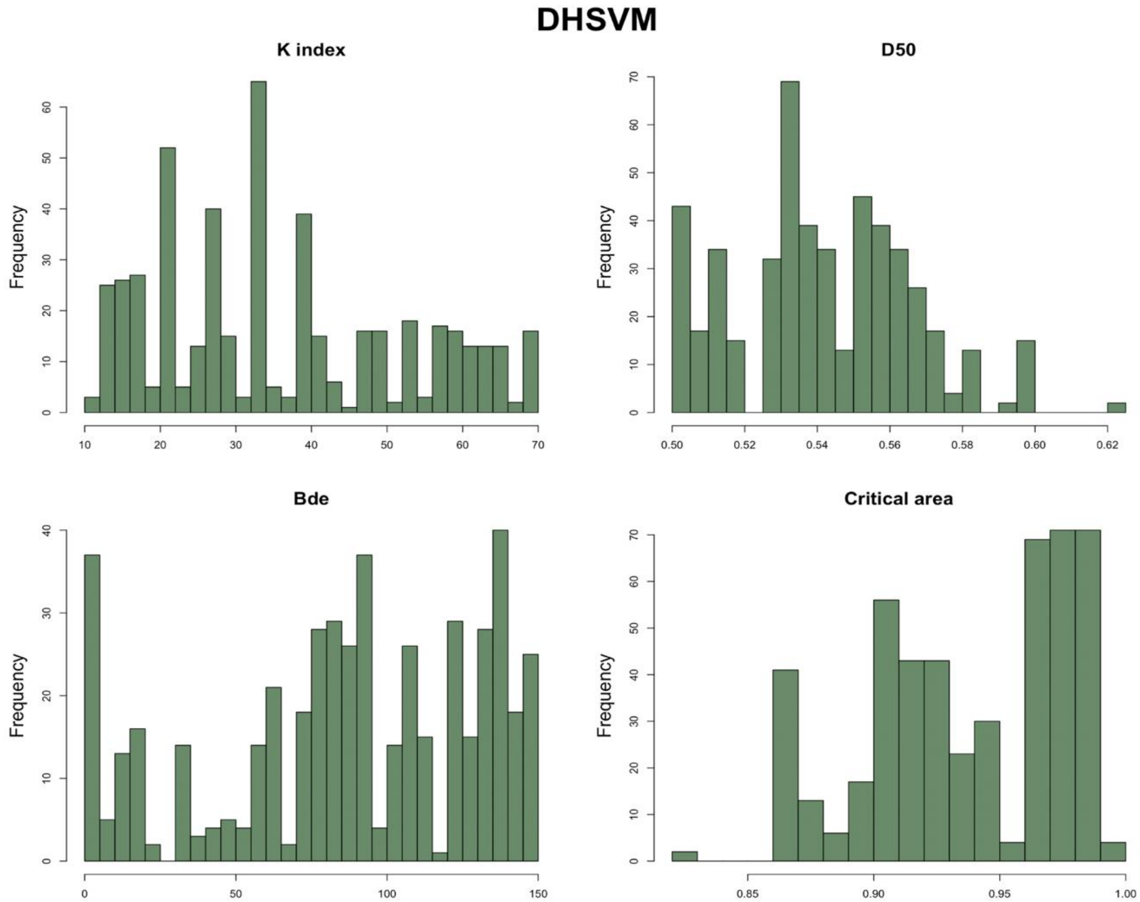

Figure 3.9: Histograms of the parameter distributions for behavioral algorithm realizations that fall within density error bars for DHSVM.

For HSPF, the parameters with dominant values are JG, JR and JS. For JG a value of 1 is most common, for JR a value between 1 and 3 is most common and for JG and for JS a value between 1 and 1.5 is most common. For JR, JS and JG there are 300 or more simulations that fall within the most common value. The maximum for other values is 50. Critical area and K factor values are skewed towards 1. P factor values peak around 0.6. KS, AFFIX and KG have random distribution across their respective ranges.

For DHSVM, only simulations with critical areas above 0.8 were within the density error bars which emphasizes that DHSVM under estimates sedimentation in the Prineville Reservoir. D50 ranges from 0.5 to 2. However only values below 0.6 resulted in simulation that had accumulated sediment with in the density error bars. Only D50 below 0.6 performed within reasonable bounds, this makes sense that it is the lower side because smaller grainsizes are able to be transported more easily.

3.6 Linear Reservoir Sediment Accumulation Analysis

3.6.1 Root Mean Squared Difference

The assumption that sediment accumulates linearly through time in reservoirs has been made in multiple past studies (Graf et al., 2010). To evaluate this assumption for the Prineville Reservoir, RMSE was calculated for yearly reservoir sediment accumulation between each algorithm realization and a comparable linear assumption with identical initial and final accumulated sediment values. (See section 2.6 for clarification.) While the term RMSE is used, we are effectively concerned in the Root Mean Squared Difference to characterize the deviation between each algorithm and a linear assumption of reservoir sediment accumulation, rather than to discuss error. Figure 3.10. shows histograms for each algorithm of yearly RMSE and table 3.1 conveys the deviation between the linear estimate and simulation as a percent of the linear estimate. Only behavioral simulations are included in this analysis.

Table 3. 2: Percent yearly deviation from a linear assumption of reservoir sediment accumulation for each of the three sediment algorithms.

Algorithm	% yearly deviation
MUSLE	89.41 %
HSPF	24.32 - 41.52 %
DHSVM	45.07 %

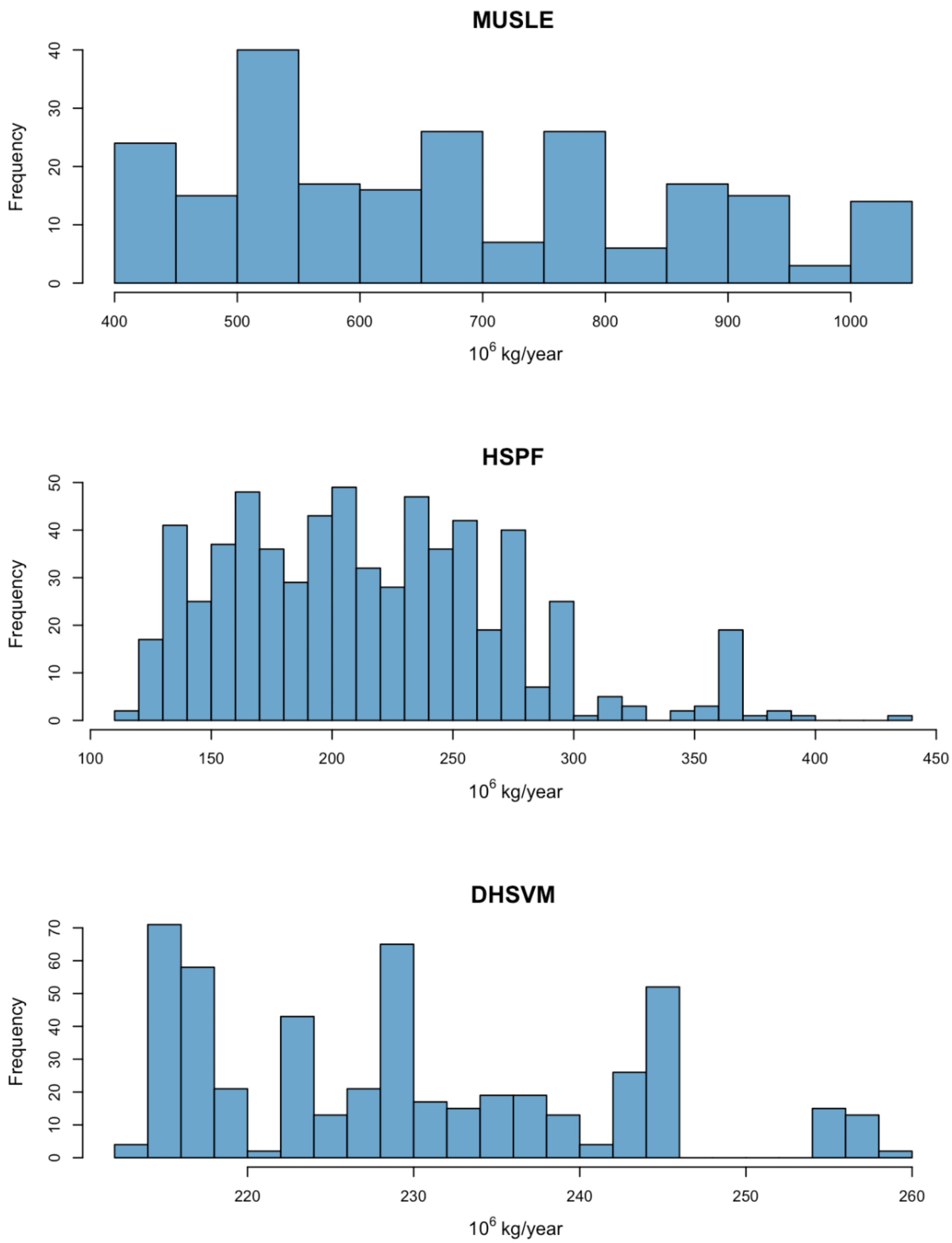

Figure 3.10: Histograms of the yearly average RMSE for comparison to a linear assumption of reservoir sediment accumulation. Smaller values indicate the simulation more similar to a linear assumption. The values represent the average sedimentation error over the period from 1960 to 1998. MUSLE has 226 data points, HSPF has 640 and DHSVM has 493.

MUSLE has the largest yearly deviation from the linear assumption at 89.41% which is followed by a 45.07% deviation for DHSVM. MUSLE and DHSVM have a small range of RMSE for their respective algorithm simulation; the values are equivalent with each other to 5 decimal places and will hereafter be referred to as the same value. The values are the same across the simulation for two reasons. First, the yield linearity analysis presented here assumes that each respective simulation results in the correct amount of reservoir sediment accumulation by the end of the run, meaning that each model simulation has a different linear function, specific that that simulations initial and final value. Secondly, the parameters varied for the Sobol analysis in MUSLE and DHSVM are linearly related to the resulting reservoir sediment accumulation.

Importantly, HSPF exhibited the most complex parameter interactions among the three algorithms (Figure 3.5). The two most sensitive parameters were the scour and detachment coefficients. These coefficients are applied as exponents, so are not linearly related to the resulting reservoir sediment accumulation. Therefore, the HSPF simulations exhibit varying degrees of deviation from the linear assumption of reservoir sediment accumulation, resulting in a range in the percent difference. The relative RMSE for HSPF, 24.32 - 41.52 %, is the lowest of the three algorithms.

When compared to the timeseries plots in 3.4, the difference from the linear estimate agrees with the results. MUSLE, which is driven by both baseflow and runoff, shows the least yield linearity because of the seasonal variation in streamflow. DHSVM and HSPF however are driven by runoff which is limited in the Crooked River basin. They both produce sediment that accumulates at a more constant rate than MUSLE.

In conclusion, these results demonstrate that the yield linearity of sediment is reliant on the streamflow regime. When modeling these processes, it is important to note how each process is incorporated into the sediment algorithms. For example, MUSLE accounts for total streamflow, so the both baseflow and runoff influence its sediment yield, whereas HSPF and DHSVM are exclusively driven by runoff. The simulated runoff in the Crooked River has a relatively steady rate, such that DHSVM and HSPF appear to have a more linear sediment yield than MUSLE.

3.6.2 Error Extrapolating Linear Projections

This section provides a comparison of sediment yield between the first 19 years and the second 19 years of the time period between the reservoir surveys in 1960 and 1998. We attempt to replicate linear yield estimates by treating the accumulated sediment yield value in 1979 as a reservoir survey. The linear slope from the first period 1960-1979 is extended to the second period 1979 to 1998 and an error between this extrapolation and the simulated value is calculated as a percent difference. The percent difference for each model is seen in table 3.3. Figure 3.11 shows histograms of the total sediment yield for each simulation in the respective time periods, 1960 to 1979 on the left in yellow and 1979 to 1998 on the right in green.

The results are similar to the results from the root mean squared error yield linearity assessment in section 3.6. It shows that the MUSLE simulations have the same percent difference, likely due to the linear relationship between the varied parameters and the sediment output. The DHSVM simulation also has the same percent difference because the parameters that are changed for the sensitivity analysis linearly influenced the sediment output. The simulations from HSPF, however, have a range of percent differences which show parameters in HSPF influence the magnitude of sediment yield rate.

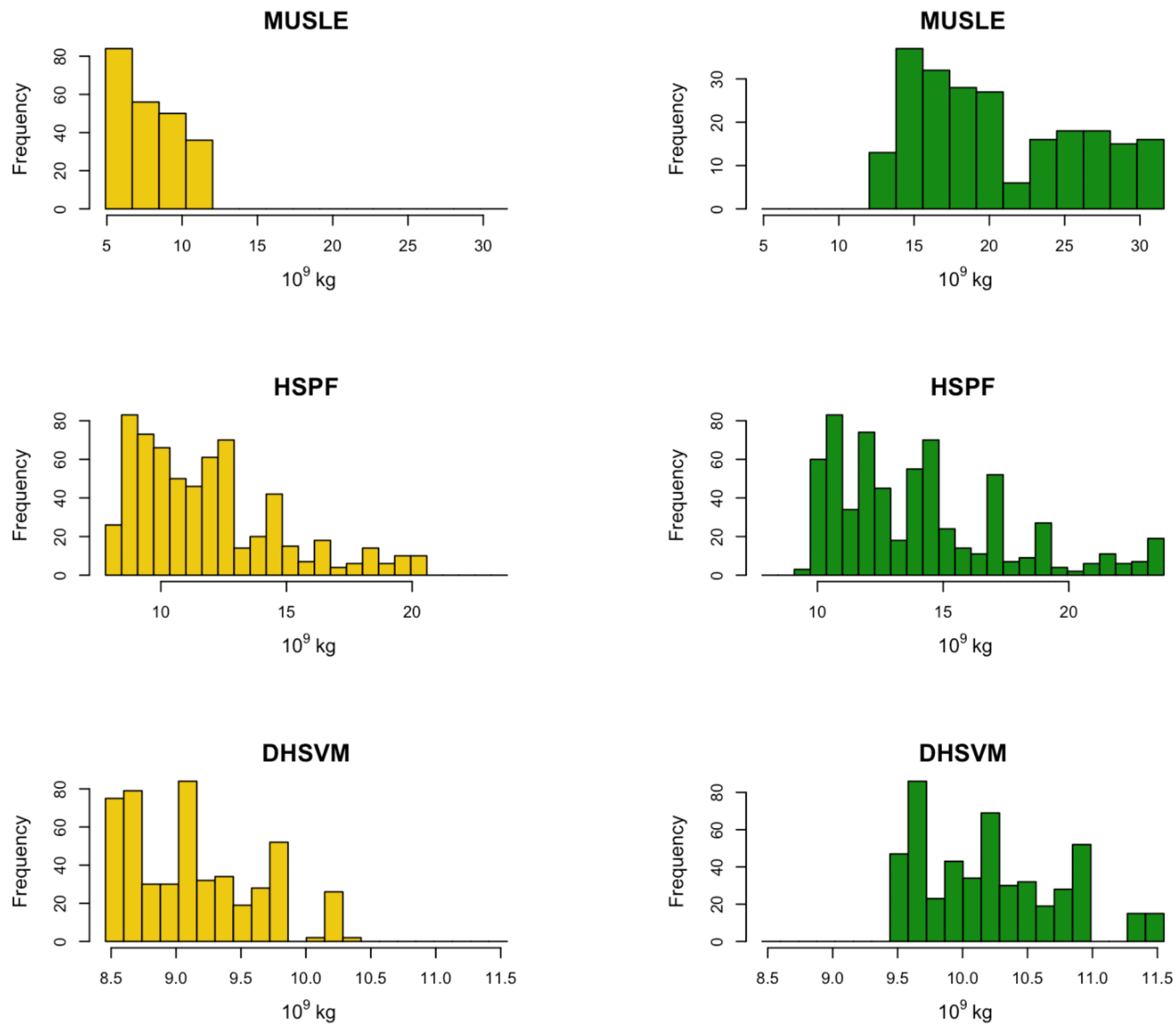

Figure 3.11: Total sediment yield for 1960 to 1979 (yellow) and 1979 to 1998 (green). Only behavioral simulations with a final total sediment yield that fell within the sediment density error bars as seen in figure 3.4 were analyzed.

Table 3.3: Percent difference between the total sediment yield from 1960 to 1979 and 1979 to 1998.

Algorithm	**Difference**
MUSLE	164.17%
HSPF	11.9% to 34.00%
DHSVM	11.84%

Chapter 4 Discussion & Conclusion

Overview

As reservoir infrastructure in the United States continues to age, fill with sediment and be stressed by climate change, it is increasingly important to understand the processes behind sedimentation. The available reservoir volume surveys are too infrequent for understanding climate-driven changes in sedimentation rates. Hydrologically forced algorithms offer a way to inform process-level understanding of sedimentation drivers. Yet, few sediment algorithms have been applied to the problem of reservoir sedimentation and an ensemble of algorithms have hitherto not been brought to bear on this problem. We applied the hydrologically forced sediment algorithm ensemble developed by Stewart et al., (2017) that includes physically-based, conceptual, and empirical algorithms, to the Crooked River watershed which feeds Prineville Reservoir near Bend, OR. Through a Sobol sensitivity analysis we aimed to address the following questions:1) Can hydrologically-forced sediment algorithms help us advance reservoir sedimentation estimates to improve future planning?2) To which processes and inputs are reservoir sedimentation estimates most sensitive?
3) What can we learn from hydrologically driven algorithms that the linear sediment yield assumption fails to assess?

4.1 Streamflow Sensitivity

Parameter sensitivity for streamflow within the VIC model was evaluated with a Sobol sensitivity analysis. We found the layer 2 depth parameter was much more sensitive than other parameters which was consistent with findings of Demaria et al., (2007). The basin’s gradual snowmelt produces consistent low flows, therefore the limiting factor of infiltration is the quantity of water, not the infiltration capacity (binf). For future modeling of arid, snowmelt dominated basins the most important parameters are baseflow related. In the case of VIC, the layer 2 depths need to be carefully calibrated.

4.2 Streamflow Selection

Streamflow parameters to drive sedimentation were chosen based on objective function performance of the Sobol simulations. Initial results had poor peak flow performance for both magnitude and timing. To improve this, snow albedo parameters were adjusted. The selected parameters produced streamflow with NSE of 0.28 and a percent bias of 6.8%. Typically, for streamflow, an NSE greater than 0.5 is desired. However, the Crooked River is known to be challenging to model and our results are comparable to past studies (Mendoza et al., 2017; Turner, 2011). Most importantly, the need to change snow parameters corroborates with Houle et al., (2017) and Mendoza et al., (2015) who put forward that snow parameters are often fixed which limits model performance. They suggested that hydrologic models should have snow parameters that are easily adjusted to improve model performance.

4.3 The Linear Sediment Yield Assumption

The analysis of the difference between a linear yield assumption and the algorithms indicated that errors associated with the yield linearity assumption can range from ±25- 90% annually, depending on the chosen algorithm. MUSLE and DHSVM had differences from the linear assumption of 89.4% and 45.1%, respectively. The parameters changed in the sensitivity analysis for DHSVM and MUSLE have a linear relationship to the sediment output which results in a commensurate difference for all simulations for the respective algorithms. However, HSPF exhibited more complex parameter interactions and the most sensitive parameters (the scour coefficient and detachment coefficient) are applied as exponents. The result is that the rate of sediment yield is extremely sensitive to the value of the scour coefficient and detachment coefficient parameters. This indicates that great care must be taken in identifying their values for any applications of the sediment algorithms.

4.4 Future Work

This study investigated the physical drivers and model sensitivities for sediment algorithms MUSLE, HSPF and DHSVM. It was performed through a case study of a single reservoir, Prineville Reservoir near Bend, OR. To further evaluate sediment drivers and uses for estimating reservoir sedimentation, the analysis should be expanded to additional reservoirs across the West. In addition, future work should evaluate changing climate forcings on sediment yield.

4.5 Conclusion

We performed a case study on the Prineville reservoir that aimed to provide insight into the driving forces of sedimentation. We implemented a Sobol sensitivity analysis for both streamflow and sediment on a hydrologically forced sediment model ensemble developed by Stewart et al. (2017). The simulations from the sensitivity analysis were analyzed further to evaluate model performance.

It was found that the sediment regime relies heavily on different aspects of the streamflow regime. Models use the streamflow regime differently to force sedimentation, so model selection for sedimentation should consider the dominant processes in streamflow (i.e. runoff and/or baseflow). The commonly used linear assumption can be helpful, however it fails to assess seasonal and decadal changes in sediment yield that can cause long term errors when estimating sediment yield.

Works Cited

Alizadeh, M.J., Jafari Nodoushan, E., Kalarestaghi, N., Chau, K.W., 2017. Toward multi-day-ahead forecasting of suspended sediment concentration using ensemble models. Environ. Sci. Pollut. Res. 24, 28017–28025. https://doi.org/10.1007/s11356-017-0405-4

Annandale, G.W., Morris, G.L., Karki, P., 2016. Extending the Life of Reservoirs. World Bank, Washington, DC.

Arnold, J.G., Srinivasan, R., Muttiah, R.S., Williams, J.R., 1998. Large Area Hydrologic Modeling and Assessment Part I: Model Development1. JAWRA J. Am. Water Resour. Assoc. 34, 73–89. https://doi.org/10.1111/j.1752-1688.1998.tb05961.x

Arnold, J.G., Williams, J.R., Maidment, D.R., 1995. Continuous-Time Water and Sediment-Routing Model for Large Basins. J. Hydraul. Eng. 121, 171–183. https://doi.org/10.1061/(ASCE)0733-9429(1995)121:2(171)

Bicknell, B.R., Imhoff, J.C., Kittle, J.L., Donigian, A.S., 1996. HYDROLOGICAL SIMULATION PROGRAM - FORTRAN USER'S MANUAL FOR RELEASE 1 880.

Boyle, D.P., Gupta, H.V., Sorooshian, S., 2000. Toward improved calibration of hydrologic models: Combining the strengths of manual and automatic methods. Water Resour. Res. 36, 3663–3674. https://doi.org/10.1029/2000WR900207

Brown, C.., 1949. Sediment Transportation, in: Engineered Hyarulics. John Wiley and Sons, Inc., Hoboken, NJ.

Brune, G.M., 1953. Trap efficiency of reservoirs. Eos Trans. Am. Geophys. Union 34, 407–418. https://doi.org/10.1029/TR034i003p00407

Churchill, M.A., 1947. Discussion of "Analyses and use of Reservoir Sedimentation Data by L.C. Gottschalk." Presented at the Federal Interagency Sedimentation Conference, U.S Geological Survey, Denver, CO.

Demaria, E.M., Nijssen, B., Wagener, T., 2007. Monte Carlo sensitivity analysis of land surface parameters using the Variable Infiltration Capacity model. J. Geophys. Res. Atmospheres 112. https://doi.org/10.1029/2006JD007534

Dendy, F.E., Cooper, C.M., 1984. Sediment trap efficiency of a small reservoir. J. Soil Water Conserv. 39, 278–280.

Easterling, D.R., Evans, J.L., Groisman, P.Y., Karl, T.R., Kunkel, K.E., Ambenje, P., 2000. Observed Variability and Trends in Extreme Climate Events: A Brief Review. Bull. Am. Meteorol. Soc. 81, 417–426. https://doi.org/10.1175/1520-0477(2000)081<0417:OVATIE>2.3.CO;2

Eggers, R.J., 2003. Prineville Reservoir, Resource Management Plan 185.

Ferrari, R., L., 1999. Prineville Reservoir 1998 Sedimentation Survey. US Departmet Inter.

Gesch, D., Oimoen, M., Greenlee, S., Nelson, C., Steuck, M., Tyler, D., 2002. The National Elevation Dataset. Am. Soc. Photogramm. Remote Sens. 68, 9.

Graf, W.L., Wohl, E., Sinha, T., Sabo, J.L., 2010. Sedimentation and sustainability of western American reservoirs. Water Resour. Res. 46. https://doi.org/10.1029/2009WR008836

Gupta, H.V., Kling, H., 2011. On typical range, sensitivity, and normalization of Mean Squared Error and Nash-Sutcliffe Efficiency type metrics. Water Resour. Res. 47. https://doi.org/10.1029/2011WR010962

Gupta, H.V., Kling, H., Yilmaz, K.K., Martinez, G.F., 2009. Decomposition of the mean squared error and NSE performance criteria: Implications for improving hydrological modelling. J. Hydrol. 377, 80–91. https://doi.org/10.1016/j.jhydrol.2009.08.003

Hamlet, A.F., Lettenmaier, D.P., 2007. Effects of 20th century warming and climate variability on flood risk in the western U.S. Water Resour. Res. 43. https://doi.org/10.1029/2006WR005099
Hansen, M.C., Defries, R.S., Townshend, J.R.G., Sohlberg, R., 2000. Global land cover classification at 1 km spatial resolution using a classification tree approach. Int. J. Remote Sens. 21, 1331–1364. https://doi.org/10.1080/014311600210209
Heinemarm, H.G., 1981. A New Sediment Trap Efficiency Curve for Small Reservoirs1. JAWRA J. Am. Water Resour. Assoc. 17, 825–830. https://doi.org/10.1111/j.1752-1688.1981.tb01304.x
Himanshu, S.K., Pandey, A., Basant, Y., 2017. Ensemble Wavelet-Support Vector Machine Approach for Prediction of Suspended Sediment Load Using Hydrometeorological Data. J. Hydrol. Eng. 22, 05017006. https://doi.org/10.1061/(ASCE)HE.1943-5584.0001516
Houle, E.S., Livneh, B., Kasprzyk, J.R., 2017. Exploring snow model parameter sensitivity using Sobol' variance decomposition. Environ. Model. Softw. 89, 144–158. https://doi.org/10.1016/j.envsoft.2016.11.024
Inman, D.L., Jenkins, S.A., 1999. Climate Change and the Episodicity of Sediment Flux of Small California Rivers. J. Geol. 107, 251–270. https://doi.org/10.1086/314346
Johanson, R.C., Davis, H.H., Incorporated, H., Branch, U.S.R.L. (Athens, Ga).Technology Development and Applications, Ga.), E.R.L. (Athens, 1980. Users Manual for Hydrological Simulation Program - FORTRAN (HSPF). Environmental Research Laboratory, Office of Research and Development, U.S. Environmental Protection Agency.
Jothiprakash, V., Garg, V., 2009. Reservoir Sedimentation Estimation Using Artificial Neural Network. J. Hydrol. Eng. 14, 1035–1040. https://doi.org/10.1061/(ASCE)HE.1943-5584.0000075
Julien, P.Y., 2010. Erosion and Sedimentation (2nd Edition). Cambridge University Press.
Knighton, D., 2014. Fluvial Forms and Processes : A New Perspective. Routledge. https://doi.org/10.4324/9780203784662
Kondolf, G.M., Gao, Y., Annandale, G.W., Morris, G.L., Jiang, E., Zhang, J., Cao, Y., Carling, P., Fu, K., Guo, Q., Hotchkiss, R., Peteuil, C., Sumi, T., Wang, H.-W., Wang, Z., Wei, Z., Wu, B., Wu, C., Yang, C.T., 2014. Sustainable sediment management in reservoirs and regulated rivers: Experiences from five continents. Earths Future 2, 256–280. https://doi.org/10.1002/2013EF000184
Liang, X., Lettenmaier, D.P., Wood, E.R., Burges, S.J., 1994. A simple hydrologically based model of land surface water and energy fluxes for general circulation models. J. Geophys. Res. Atmospheres 99, 14415–14428. https://doi.org/10.1029/94JD00483
Livneh, B., Bohn, T.J., Pierce, D.W., Munoz-Arriola, F., Nijssen, B., Vose, R., Cayan, D.R., Brekke, L., 2015. A spatially comprehensive, hydrometeorological data set for Mexico, the U.S., and Southern Canada 1950–2013. Sci. Data 2, 150042. https://doi.org/10.1038/sdata.2015.42
Livneh, B., Rosenberg, E.A., Lin, C., Nijssen, B., Mishra, V., Andreadis, K.M., Maurer, E.P., Lettenmaier, D.P., 2013. A Long-Term Hydrologically Based Dataset of Land Surface Fluxes and States for the Conterminous United States: Update and Extensions. J. Clim. 26, 9384–9392. https://doi.org/10.1175/JCLI-D-12-00508.1
Maidment, D.R., 1993. HANDBOOK OF HYDROLOGY. McGraw-Hill, New York.

Maurer, E.P., Wood, A.W., Adam, J.C., Lettenmaier, D.P., Nijssen, B., 2002. A Long-Term Hydrologically Based Dataset of Land Surface Fluxes and States for the Conterminous United States. J. Clim. 15, 3237–3251. https://doi.org/10.1175/1520-0442(2002)015<3237:ALTHBD>2.0.CO;2

McCuen, R.H., Knight Zachary, Cutter A. Gillian, 2006. Evaluation of the Nash–Sutcliffe Efficiency Index. J. Hydrol. Eng. 11, 597–602. https://doi.org/10.1061/(ASCE)1084-0699(2006)11:6(597)

Mendoza, P.A., Clark, M.P., Barlage, M., Rajagopalan, B., Samaniego, L., Abramowitz, G., Gupta, H., 2015. Are we unnecessarily constraining the agility of complex process-based models? Water Resour. Res. 51, 716–728. https://doi.org/10.1002/2014WR015820

Mendoza, P.A., Wood, A.W., Clark, E., Rothwell, E., Clark, M.P., Nijssen, B., Brekke, L.D., Arnold, J.R., 2017. An intercomparison of approaches for improving operational seasonal streamflow forecasts. Hydrol. Earth Syst. Sci. 21, 3915–3935. https://doi.org/10.5194/hess-21-3915-2017

Miller, D.A., White, R.A., 1998. A Conterminous United States Multilayer Soil Characteristics Dataset for Regional Climate and Hydrology Modeling. Earth Interact. 2, 1–26. https://doi.org/10.1175/1087-3562(1998)002<0001:ACUSMS>2.3.CO;2

Minear, J.T., Kondolf, G.M., 2009. Estimating reservoir sedimentation rates at large spatial and temporal scales: A case study of California. Water Resour. Res. 45. https://doi.org/10.1029/2007WR006703

Morris, G.L., Fan, J., 1998. Reservoir Sedimentation Handbook: design and managment of dams, reervoirs and watersheds for sustainable use. McGraw Hill Professional.

Nash, J.E., Sutcliffe, J.V., 1970. River flow forecasting through conceptual models part I — A discussion of principles. J. Hydrol. 10, 282–290. https://doi.org/10.1016/0022-1694(70)90255-6

Nossent, J., Bauwens, W., 2012. Optimising the convergence of a Sobol' sensitivity analysis for an environmental model: application of an appropriate estimate for the square of the expectation value and the total variance. Sensit. Anal. 9.

Nossent, J., Elsen, P., Bauwens, W., 2011. Sobol' sensitivity analysis of a complex environmental model. Environ. Model. Softw. 26, 1515–1525. https://doi.org/10.1016/j.envsoft.2011.08.010

Odhiambo, B.K., Boss, S.K., 2004. Integrated Echo Sounder, Gps, and Gis for Reservoir Sedimentation Studies: Examples from Two Arkansas Lakes1. JAWRA J. Am. Water Resour. Assoc. 40, 981–997. https://doi.org/10.1111/j.1752-1688.2004.tb01061.x

Pagano, T., Garen, D., Sorooshian, S., 2004. Evaluation of Official Western U.S. Seasonal Water Supply Outlooks, 1922–2002. J. Hydrometeorol. 5, 896–909. https://doi.org/10.1175/1525-7541(2004)005<0896:EOOWUS>2.0.CO;2

Palmieri, A., Shah, F., Dinar, A., 2001. Economics of reservoir sedimentation and sustainable management of dams. J. Environ. Manage. 61, 149–163. https://doi.org/10.1006/jema.2000.0392

Pierce, D.W., Barnett, T.P., Hidalgo, H.G., Das, T., Bonfils, C., Santer, B.D., Bala, G., Dettinger, M.D., Cayan, D.R., Mirin, A., Wood, A.W., Nozawa, T., 2008. Attribution of Declining Western U.S. Snowpack to Human Effects. J. Clim. 21, 6425–6444. https://doi.org/10.1175/2008JCLI2405.1

Podolak, C.J.P., Doyle, M.W., 2015. Reservoir Sedimentation and Storage Capacity in the United States: Management Needs for the 21st Century. J. Hydraul. Eng. 141, 02515001. https://doi.org/10.1061/(ASCE)HY.1943-7900.0000999
Randle, T.J., Bountry, J., 2016. Dam Removal Analysis Gruidlines For Sediment. Bur. Reclam.
Saltelli, A., 2002. Making best use of model evaluations to compute sensitivity indices. Comput. Phys. Commun. 145, 280–297. https://doi.org/10.1016/S0010-4655(02)00280-1
Sankey, J.B., Kreitler, J., Hawbaker, T.J., McVay, J.L., Miller, M.E., Mueller, E.R., Vaillant, N.M., Lowe, S.E., Sankey, T.T., 2017. Climate, wildfire, and erosion ensemble foretells more sediment in western USA watersheds. Geophys. Res. Lett. 44, 8884–8892. https://doi.org/10.1002/2017GL073979
Sobol, I.., 2001. Global sensitivity indices for nonlinear mathematical models and their Monte Carlo estimates. Math. Comput. Simul. 55, 271–280. https://doi.org/10.1016/S0378-4754(00)00270-6
Sobol, I.M., 1976. Uniformly distributed sequences with an additional uniform property. USSR Comput. Math. Math. Phys. 16, 236–242. https://doi.org/10.1016/0041-5553(76)90154-3
Sohoulande Djebou, D.C., 2018. Assessment of sediment inflow to a reservoir using the SWAT model under undammed conditions: A case study for the Somerville reservoir, Texas, USA. Int. Soil Water Conserv. Res. 6, 222–229. https://doi.org/10.1016/j.iswcr.2018.03.003
Stewart, J., 2017. A Multi-Algorithm Approach to Suspended Sediment Modeling in the Colorado Front Range. Civ. Eng. Grad. Theses Diss.
Stewart, J., Rajagopalan, B., Kasprzyk, J., Raseman, W., Livneh, B., 2017. The Use of Ensemble Modeling of Suspended Sediment to Characterize Uncertainty. American Society of Civil Engineers, pp. 207–218. https://doi.org/10.1061/9780784480625.019
Stewart, J.R., Livneh, B., Kasprzyk, J.R., Rajagopalan, B., Minear, J.T., Raseman, W.J., 2017. A Multialgorithm Approach to Land Surface Modeling of Suspended Sediment in the Colorado Front Range. J. Adv. Model. Earth Syst. 9, 2526–2544. https://doi.org/10.1002/2017MS001120
Tang, Y., Reed, P., van Werkhoven, K., Wagener, T., 2007. Advancing the identification and evaluation of distributed rainfall-runoff models using global sensitivity analysis: DISTRIBUTED MODEL SENSITIVITY ANALYSIS. Water Resour. Res. 43. https://doi.org/10.1029/2006WR005813
Turner, T., 2011. Climate and Hydrology Datasets for Use in the MRJOC Agencies' Longer-Term Planning Studies Part II. US Bur. Reclam.
U.S. Bureau of Reclamation, 2016. Hydromet Pacific Northwest Region [WWW Document]. URL https://www.usbr.gov/pn/hydromet/arcread.html (accessed 8.30.18).
U.S. Geological Survey, 2016. National Water Information Systems data availible on the World Wide Web (USGS Water Data for the Nation) [WWW Document]. URL https://waterdata.usgs.gov/nwis/inventory/?site_no=14080500 (accessed 8.30.18).
U.S. Geological Survey Water Information Coordination Program, 2014. The Reservoir Sedimentation Database (RESSED) [WWW Document]. URL https://water.usgs.gov/osw/ressed/index.html (accessed 8.30.18).
van Werkhoven, K., Wagener, T., Reed, P., Tang, Y., 2008. Characterization of watershed model behavior across a hydroclimatic gradient: WATERSHED MODEL BEHAVIOR. Water Resour. Res. 44. https://doi.org/10.1029/2007WR006271

Wagener, T., Kollat, J., 2007. Numerical and visual evaluation of hydrological and environmental models using the Monte Carlo analysis toolbox. Environ. Model. Softw. 22, 1021–1033. https://doi.org/10.1016/j.envsoft.2006.06.017

Wicks, J.M., 1988. Physically-based mathematical modelling of catchment sediment yield. Newcastle University.

Wicks, J.M., Bathurst, J.C., 1996. SHESED: a physically based, distributed erosion and sediment yield component for the SHE hydrological modelling system. J. Hydrol. 175, 213–238. https://doi.org/10.1016/S0022-1694(96)80012-6

Wigmosta, M.S., Vail, L.W., Lettenmaier, D.P., 1994. A distributed hydrology-vegetation model for complex terrain. Water Resour. Res. 30, 1665–1679. https://doi.org/10.1029/94WR00436

Williams, J.., Berndt, H.D., 1977. Sediment yield prediction based on watershed hydrology. Trans. ASAE Am. Soc. Agric. Eng.

Wolman, M.G., 1967. A Cycle of Sedimentation and Erosion in Urban River Channels. Geogr. Ann. Ser. Phys. Geogr. 49, 385–395. https://doi.org/10.1080/04353676.1967.11879766

Yan, B., Fang, N.F., Zhang, P.C., Shi, Z.H., 2013. Impacts of land use change on watershed streamflow and sediment yield: An assessment using hydrologic modelling and partial least squares regression. J. Hydrol. 484, 26–37. https://doi.org/10.1016/j.jhydrol.2013.01.008

Zadeh, F.K., 2015. FARKHONDEH KHORASHADI ZADEH (1), FANNY SARRAZIN (2), JIRI NOSSENT (1,3), FRANCESCA PIANOSI (2), ANN VAN GRIENSVEN (1,4), THORSTEN WAGENER (2,5) & WILLY BAUWENS (1) 5.